Contact metamorphism of Fe- and Al-rich graphitic metapelites in the Transangarian region of the Yenisei Ridge, Eastern Siberia, Russia

Article *in* Lithos · February 2001

DOI: 10.1016/S0024-4937(01)00048-2

CITATIONS
65

READS
1,757

5 authors, including:

Igor Likhanov
Sobolev Institute of Geology and Mineralogy
179 PUBLICATIONS **1,741** CITATIONS

SEE PROFILE

Reverdatto Vladimir
Sobolev Institute of Geology and Mineralogy
238 PUBLICATIONS **2,005** CITATIONS

SEE PROFILE

P. S. Kozlov
Институт геологии и минералогии Сибирского отделени...
57 PUBLICATIONS **770** CITATIONS

SEE PROFILE

ELSEVIER

Lithos 58 (2001) 55–80

LITHOS

www.elsevier.com/locate/lithos

Contact metamorphism of Fe- and Al-rich graphitic metapelites in the Transangarian region of the Yenisei Ridge, eastern Siberia, Russia

I.I. Likhanov *, V.V. Reverdatto, V.S. Sheplev, A.E. Verschinin, P.S. Kozlov

Institute of Mineralogy and Petrography, Siberian Branch, Russian Academy of Sciences, Pr. Acad. Koptyuga 3, Novosibirsk 630090, Russian Federation

Received 1 August 2000; accepted 14 June 2001

Abstract

Prograde evolution of minerals in Fe- and Al-rich graphitic metapelites in the Ayakhtinsk aureole, Siberia, produced the unusual contact metamorphic mineral assemblages: chloritoid + biotite, chloritoid + biotite + andalusite and cordierite + garnet + muscovite. Field-petrologic observations show that: (1) the grade of contact metamorphism ranges from chloritoid to sillimanite–alkali feldspar zone; (2) chloritoid + biotite assemblages have a restricted temperature interval and give way up-grade to garnet + chlorite assemblages; and (3) garnet + chlorite assemblages have a wide temperature interval and give way to cordierite + biotite parageneses with increasing grade. Geothermobarometry and thermodynamic analysis of mineral equilibria give estimates of the P–T–X_{H_2O} conditions of the contact metamorphism: the temperatures increase toward the intrusive contact from 430 to 640 °C at $P = 3.2 \pm 0.3$ kbar, X_{H_2O} for the metamorphic fluid decreases toward the intrusive contact from 0.89–0.85 at $T = 450$ °C to 0.49–0.36 at $T = 640$ °C, assuming ideal and non-ideal mixing, respectively, of H_2O–CO_2 in the fluid phase. The stability of the rare mineral assemblages chloritoid + biotite and chloritoid + biotite + andalusite within the contact aureole can be explained by the unusual combination of pressure (> 3 kbar) and Fe- and Al-rich bulk-rock compositions. The local occurrence of the cordierite + garnet + muscovite mineral assemblage is controlled by Mn in the garnet composition and Fe- and Al-rich bulk-rock composition than P–T conditions. Our data are compatible with the KFMASH grid of Spear and Cheney [Contrib. Mineral. Petrol. 101 (1989) 149.].

Keywords: Contact metamorphism; Pelitic schists; Chloritoid; Yenisei Ridge

1. Introduction

Chloritoid-bearing assemblages have been described from numerous areas of regional metamorphism (e.g. Halferdahl, 1961; Holdaway, 1978; Labotka, 1981; Evirgen and Ashworth, 1984; Dickenson, 1988) as well as from a few contact aureoles (Pattison and Tracy, 1991). Nevertheless, chloritoid-bearing assemblages are not abundant in typical contact aureoles due, in part, to a narrow temperature interval at low pressures of thermal metamorphism (Ganguly, 1969) and severe constraints imposed by specific bulk rock composition (Hoschek, 1969; Albee, 1972; Wang and Spear, 1991). Previous studies, as applied to contact metamorphism, (e.g. Atherton,

* Corresponding author. Fax: +7-3832-332792.
E-mail address: likh@uiggm.nsc.ru (I.I. Likhanov).

0024-4937/01/$ - see front matter
PII: S0024-4937(01)00048-2

1980; Naggar and Atherton, 1970; Phillips, 1987; Kaneko and Miyano, 1990; Flinn et al., 1996) that have dealt with the investigation of the equilibrium relations of chloritoid with respect to the coexisting natural assemblages have provided valuable information on the chemistry, mineralogy and natural occurrence of these rocks to understanding the reactions controlling the appearance/disappearance of chloritoid-bearing assemblages during contact metamorphism of specific terranes. However, few detailed mineral chemical studies of chloritoid-bearing assemblages across contact-metamorphic isograds have been made. Consequently, we undertook a mineral chemical study of Fe- and Al-rich hornfelses near a granite intrusive in order to ascertain the formation conditions of contact-metamorphic assemblages in the thermal aureole of the Ayakhtinsk intrusive complex, Eastern Siberia, which allows the reconstruction of the P–T–X_{H_2O} mineral reaction evolution. This area was chosen for a number of reasons. First, the contact aureole developed in response to an isobaric thermal overprint by a granite intrusion; variations in phase relations and compositions are assumed to be primarily a function of changes in temperature at constant bulk rock composition. Second, the stability of the relatively rare mineral assemblages chloritoid + biotite, chloritoid + biotite + andalusite, and cordierite + garnet + muscovite within the contact aureole makes these hornfelses of particular interest. As Droop and Harte (1995) have shown, only three known occurrences of chloritoid + biotite + andalusite mineral assemblage in contact aureoles have been described in the literature: the Tono aureole, Japan (Okuyama-Kusunose, 1994); the Karatash aureole, Russia (Likhanov, 1988a); and the Insch aureole, Scotland (Nockolds et al., 1978). Cordierite + garnet + muscovite is also a rare assemblage in low-pressure contact metamorphic rocks, having been noted only in five contact aureoles (Pattison and Tracy, 1991). Thirdly, the chloritoid + biotite paragenesis has always been problematic in the construction of petrogenetic grids for pelites, in which this assemblage has markedly different stability limits. One is based on the KFMASH grid of Harte and Hudson (1979), in which chloritoid + biotite is stable over a narrow temperature interval at relatively low pressure, and the other on the KFMASH grids of Spear and Cheney (1989) and Wang and Spear (1991), in which this assemblage is stable over wide ranges of pressure and temperature. In addition, there has been a diversity of opinion on the P–T orientation of chloritoid + biotite = garnet + chlorite reaction curve. Spear and Cheney's grid predicts that garnet + chlorite is stable on the high temperature side of this reaction, whilst Harte and Hudson's grid shows the opposite. The petrological study presented below provides a good opportunity to assess the validity of these alternative petrogenetic grids for pelites. A general criticism of many existing grids is that they provide poor models for mineral assemblages in the low-pressure part of P–T space, corresponding to the studied hornfelses (Pattison and Tracy, 1991).

2. Geological setting and mineral assemblages

The study area is a contact aureole surrounding the Ayakhtinsk granite massif in the Transangarian region of the Yenisei Ridge in Eastern Siberia (Fig. 1). The Ayakhtinsk granite massif outcrops over an elliptical area measuring approximately 12×18 km., elongated in a N–W direction. The massif is composed chiefly of the Precambrian (Late Riphean) plagioclase-microcline granites with a Rb–Sr whole-rock age of 850 ± 50 Ma (Dazenko, 1984). The granites are composed of quartz (25–35 modal%), microcline (20–30 modal%), plagioclase (30–45 modal%), biotite + hornblende 5–8 modal%) and accessory zircon and apatite. Contact metamorphism was caused by intrusion of the granites into Middle Riphean country rocks of the Udereysk Formation. The contacts with the country rocks are sharp and discordant. The country rocks are a grey to black, highly schistose graphitic pelitic phyllite interbedded with thin psammitic and quartzitic layers that are remarkably uniform both in lithology and chemical composition (Likhanov et al., 1998, 2000). In the study area at the northern contact (Fig. 1), host rocks are regionally metamorphosed to greenschist facies conditions and consist of muscovite–chlorite–albite–quartz–rutile metapelites.The contact metamorphic effects of the Ayakhtinsk intrusive complex on the graphite-bearing pelitic schists are first perceptible through the first appearance of chloritoid. The thermal aureole, as defined by the chloritoid-in isograd,

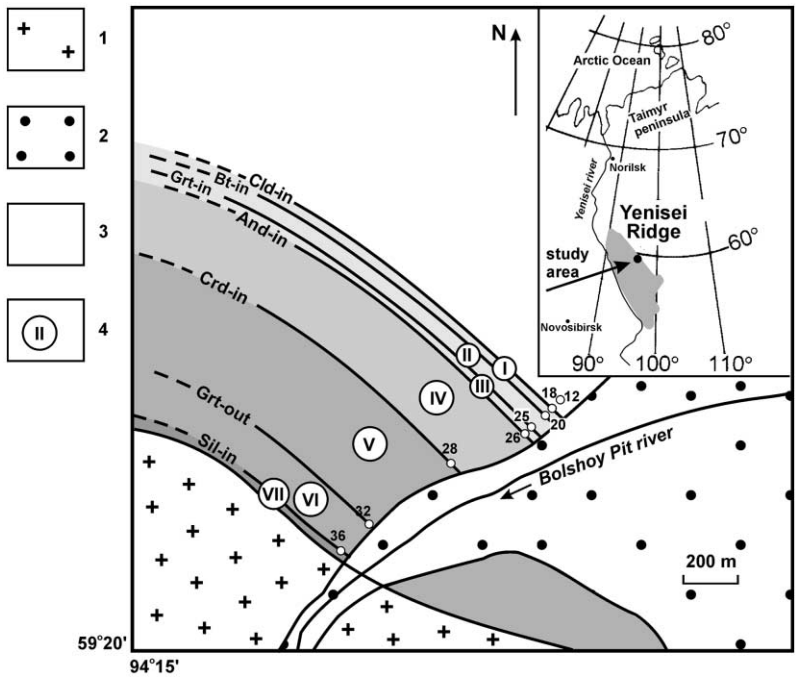

Fig. 1. Part of the northern part of the contact aureole of the Ayakhtinsk granite intrusion: (1) granites; (2) alluvium; (3) country rocks; (4) metamorphic zones: (I) chloritoid, (II) biotite, (III) garnet, (IV) andalusite, (V) lower cordierite, (VI) upper cordierite and (VII) sillimanite-alkali feldspar. Open circles are sample locations. On the inset map, the shaded area is the Yenisei Ridge, and the study area is in the solid dot.

extends 1 km to the north of the granite massif (Fig. 1) with distinct zonation due to changing hornfels structure and mineral assemblages. Based on detailed mapping and petrography, the following zones can be delineated within the country rocks and contact aureole with decreasing distance toward the granitic contact (in parenthesis—zone designation and observed thickness).

1. Chl + Ms + Pl + Qtz + Rut (country rocks)
2. Cld + Ms + Chl + Pl + Qtz + Ilm ± Rut (I—chloritoid zone, 45 m)
3. Bt + Cld + Ms + Chl + Pl + Qtz + Ilm (II—biotite zone, 60 m)
4. Grt + Bt + Cld + Ms + Chl + Pl + Qtz + Ilm (III—garnet zone, 35 m)
5. And + Bt + Grt + Ms + Chl + Pl + Qtz + Ilm ± Cld (IV—andalusite zone, 300 m)
6. Crd + And + Bt + Ms + Pl + Qtz + Ilm + Chl + Grt (V—lower cordierite zone, 400 m)
7. Crd + And + Bt + Ms + Pl + Qtz + Ilm (VI—upper cordierite zone, 150 m)
8. Sil + Kfs + Crd + Bt + Pl + Qtz + Ilm ± Ms ± And (VII—sillimanite–alkali feldspar zone, 10 m)

Symbol (±) denotes a disappearance of mineral phase in the lower grade part of the indicated zone. The assemblages listed here are the assemblages with the maximum number of phases in these zones. Common accessory minerals include graphite, tourmaline, zircon and apatite. Abbreviations for the mineral names are adopted from Kretz (1983).

3. Metamorphic zones, isograds and textural observations

Within a distance of 1 km from granite contact, it is possible to recognize and map in the field eight metamorphic zones (1–8) and seven distinct isograds. The isograds are defined in the sense discussed by Carmichael (1978); they are traces of the

surfaces marking a change in metamorphic mineralogy. The rocks of the study area interpreted have approached equilibrium based on criteria presented by Vernon (1977). The observed equilibrium relations of contact metamorphic minerals with respect to the coexisting mineral assemblages in each zone are presented graphically on a series of AFM projections (Thompson, 1957) in Fig. 2. All phases represented in the topologies shown are in contact with one another and show no evidence of replacement (except in the case of secondary chlorite formed as an alteration of biotite, and locally, as rims on garnet); grain boundaries are sharp and regular. Retrograde reaction textures are observed mainly in the andalusite and lower cordierite zones, and are absent or only a trace constituent in other zones. The AFM topology changes observed from one metamorphic zone to another may be mapped as isograds and related by a series of isogradic reactions.

The observed mineral assemblages in the hornfelses on which the zones are based are (in addition to muscovite, quartz and plagioclase): Cld + Chl (chloritoid zone), Cld + Chl + Bt, Cld + Bt (biotite zone), Grt + Cld + Chl, Grt + Bt + Chl, Grt + Chl (garnet zone), And + Grt + Cld, And + Cld + Chl, And + Chl + Bt, And + Grt + Bt, Grt + Cld + Bt, And + Bt, Cld + Bt + And, And + Bt + Grt + Chl + Cld (andalusite zone), And + Bt + Crd, Grt + Crd + And, Grt + Crd + Bt, Crd + Bt + Chl, Grt + Chl + Bt, Crd + Grt, Grt + And + Crd + Bt + Chl (lower cordierite zone), And + Bt + Crd, Crd + And, Crd + Bt (upper cordierite zone), and Crd + Sil + Kfs, Crd + Sil + Bt, And + Sil + Crd + Kfs, And + Kfs + Bt (sillimanite–alkali feldspar zone). Each assemblage reflects a peak metamorphic association of minerals within a single thin section. Assemblages of four and five 'AFM' minerals are confirmed where the constituent minerals are found close together or

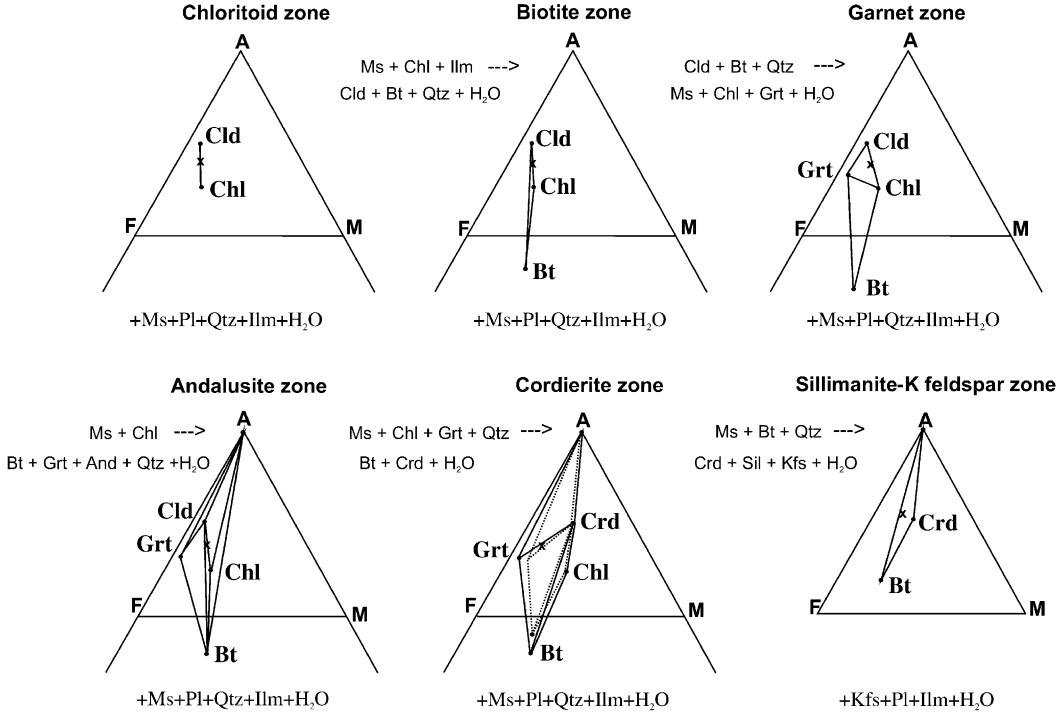

Fig. 2. Schematic AFM diagrams representing observed mineral assemblages and progressive metamorphism of pelitic hornfelses in the Ayakhtinsk contact aureole. For the Sil–Kfs zone projection constructed from Kfs, Pl, Ilm and fluid of fixed a_{H_2O}; for all other zones—from Ms, Qtz, Pl, Ilm and fluid of fixed a_{H_2O}. Bulk rock and mineral compositions are shown as crosses and points, respectively. The observed mineral assemblages of the upper cordierite zone indicate by dotted lines.

occur in several combinations of two- and three-phase subassemblages within a single thin section.

The rocks farthest removed from the intrusive contact, namely the chloritoid, biotite and garnet zones, preserve most of their pre-contact metamorphic features, such as clastic grains, relict phyllitic texture and schistosity. These low-grade rocks differ from the country rock phyllites only by virtue of their more compact structure and the presence of chloritoid, biotite and garnet. Typical low-grade indurated schists are lepidoblastic, micro- or fine-grained rocks. The first new phases to appear in the contact aureole are chloritoid and ilmenite (chloritoid-in isograd). Euhedral prismatic and tabular crystals (up to 1.5 mm) of chloritoid are randomly orientated at a steep angle to the foliation and overgrew this foliation. In thin section, these crystals are often twinned and have the hourglass structure (Fig. 3). Sector zoning of chloritoid is indicated by the presence of graphite-bearing and graphite-free areas. Graphite is the most abundant accessory mineral in all rocks of the contact aureole. It usually occurs as fine-grained particles, up to 0.1 mm across, disseminated in the rock matrix. Rutile appears to be replaced by ilmenite since some of the ilmenite laths have thin lamellae of rutile. Biotite first occurs at the biotite-in isograd in fine flakes that are up to 0.5 mm in length in the lepidogranoblastic, fine-grained matrix which consists of recrystallized aggregates of muscovite–chlorite–plagioclase–quartz with opaque minerals. Biotite is often in contact with chloritoid. Garnet-bearing assemblages first appear at the garnet-in isograd. The garnets are small idiomorphic porphyroblasts with abundant inclusions of chloritoid and quartz and few inclusions of biotite and ilmenite, and are generally less than 0.5–1 mm across. The garnet modal abundance seldom exceeds 3% of the rock volume. Micas, chlorite, chloritoid and quartz constitute the matrix.

The andalusite zone is bounded on the high-grade side by the cordierite-in isograd. Poikiloblastic and subhedral andalusite crystals up to 2 mm across with irregular and ovoid margins (Fig. 4) overprint the pre-existing foliation of country rocks and produce the spotted texture in low-grade spotted schists of the andalusite zone. With increasing grade, andalusite modal abundance (by visual estimate) and grain size (up to 5 mm) generally increase. Approaching the

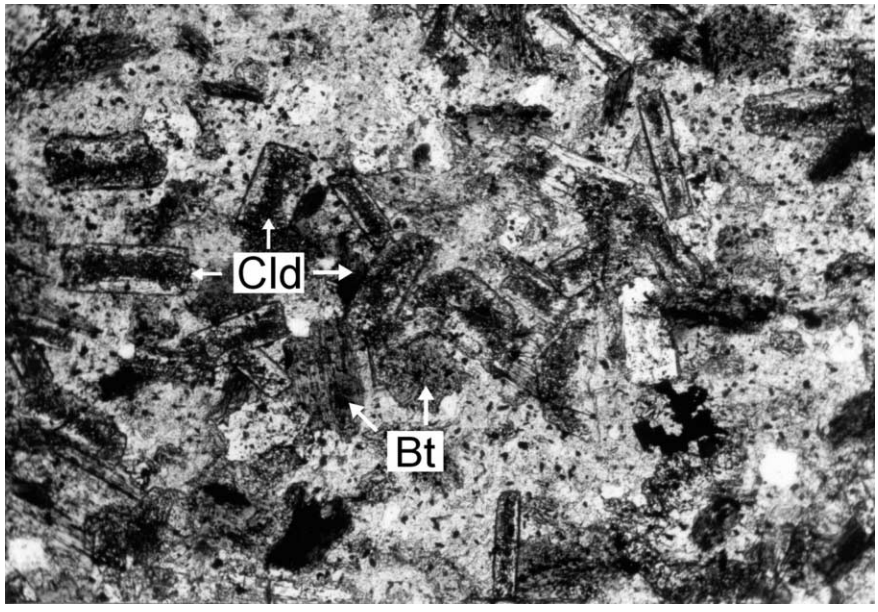

Fig. 3. Chloritoid-biotite schist with biotite flakes and prismatic, commonly twined, chloritoid crystals with the hourglass structure. Biotite zone, Sample 20, plane-polarized light. Long axis of the photomicrograph is 8 mm.

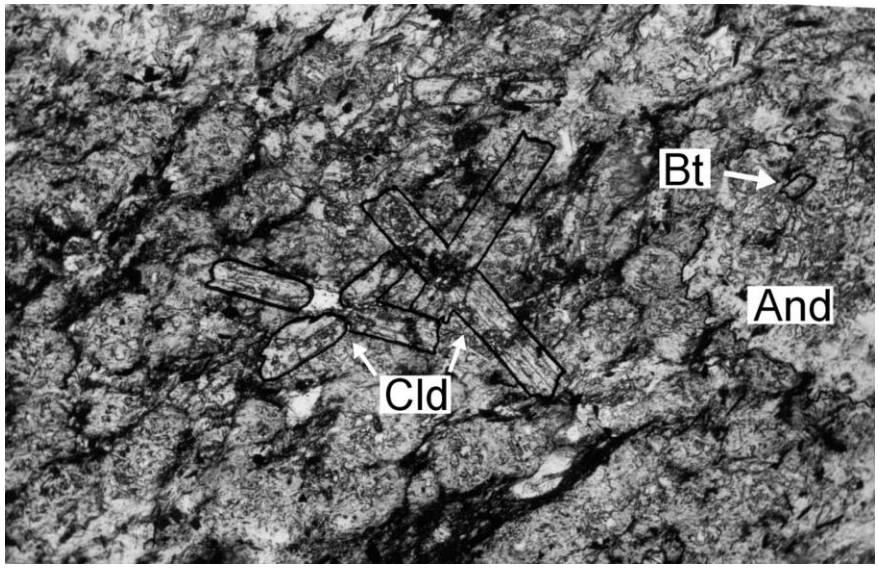

Fig. 4. Cruciform penetration twin of chloritoid with poikiloblastic and subhedral andalusite crystals, containing small flakes of biotite, with irregular margins in a chlorite–muscovite matrix. Andalusite zone, Sample 26, plane-polarized light. Long axis of the photomicrograph is 8 mm.

cordierite-in isograd, the pelitic rocks of the andalusite zone develop decussate texture with random orientation of minerals, characteristic of low/intermediate-grade hornfelses. The rare mineral assemblage chloritoid + biotite + andalusite occurs within the andalusite zone of the contact aureole. Above the andalusite-in isograd chlorite and muscovite continue to decrease in modal amount. Going upgrade through andalusite zone, the chloritoid abruptly decreases in modal amount and disappears near the cordierite-in isograd. The garnets are larger (up to 1.5-mm diameter) and more abundant than in garnet zone, but the modal abundance seldom exceed 5% of the rock volume.

Metamorphic rocks of the cordierite zone are completely recrystallized to fine-grained hornfels. All aspects of regional metamorphism are obliterated. The area between the cordierite-in isograd and the sillimanite-in isograd has been divided into lower and upper cordierite zones. Typical cordierite-bearing hornfelses are massive, dense, fine-grained rocks that break with a distinctive conchoidal fracture. In thin section, they show granoblastic texture. Cordierite occurs as ellipsoidal, inclusion-filled anhedral poikiloblasts, from 1.5 up to 3 mm in diameter, accompanied by randomly oriented biotite, muscovite and andalusite crystals. Common inclusions in the cordierites are chlorite and muscovite. The rare mineral assemblage cordierite + garnet + muscovite occurs within the lower cordierite zone. As the granitic contact is approached, the last traces of chlorite and garnet disappear in the rocks of the lower cordierite zone, which marks the beginning of the upper cordierite zone. Above the garnet- and chlorite-out isograd, cordierite continues to increase in amount while muscovite and andalusite decrease.

The appearance of sillimanite and alkali feldspar marks the beginning of the sillimanite–alkali feldspar zone, the higher grade zone in the aureole. Below this zone, andalusite is the only Al_2SiO_5 polymorph present. Andalusite and sillimanite occur together in some samples near the sillimanite–alkali feldspar isograd, but sillimanite does not appear to nucleate on andalusite thus providing no evidence for the direct replacement of andalusite by sillimanite. Some samples contain randomly orientated sillimanitic sprays occur adjacent to cordierite crystals and alkali feldspar in a matrix of quartz, muscovite, ilmenite, plagioclase and locally biotite. Sillimanite also occurs as fibrolitic aggregates, forming knots of tiny

fibres overgrowing biotite and muscovite. Andalusite forms in two main habits: anhedral, skeletal crystals and mosaic crystal aggregates, surrounded by K-feldspar and biotite. Going upgrade through sillimanite–alkali feldspar zone up to the igneous contact, sillimanite is found without associated andalusite and is the only Al_2SiO_5 polymorph present. An abrupt decrease of muscovite, andalusite and quartz coincides with the abundance and grain size of sillimanite increase in the highest grade samples. Typical textural and structural features of the sillimanite–alkali feldspar zone hornfelses are indistinguishable from the hornfelses of the cordierite zone.

4. Bulk rock chemistry and isochemical nature of contact metamorphism

Bulk-rock analyses were obtained by XRF, with the VRA-20 energy dispersive spectrometer, in the United Institute of Geology, Geophysics and Mineralogy, Novosibirsk (Table 1). Thirty-five bulk-rock analyses were made of the most representative different rocks across the contact aureole and from country rocks. The probed rocks selected for bulk-chemical analysis contain the mineral assemblages typical of the zones from which they were sampled. Seventeen of these samples belong to the country schists prior outside the contact metamorphic aureole and eighteen to the hornfelses. As concerns Table 1, the rocks enclosing the massif are homogeneous graphite-bearing pelitic schists with a narrow range of high-Fe ($X_{Fe} = FeO/(FeO + MgO + MnO) =$ 0.72–0.74 whole rock on a mole basis) and high-Al ($X_{Al} = (Al_2O_3 - 3K_2O - Na_2O)/(Al_2O_3 - 3K_2O - Na_2O + FeO + MgO + MnO) = 0.30–0.32$) bulk compositions as compared with the average pelite whole-rock composition ($X_{Fe} = 0.52$ and $X_{Al} = 0.13$) (Shaw, 1956; Symmes and Ferry, 1992) and plot above the garnet–chlorite tie-line in AFM (Fig. 2). The bulk-rock Mn-content of pelitic schists ($X_{Mn} = MnO/(MnO + FeO + MgO)$) varies from 0.017 to 0.025 (0.24–0.36 wt.% MnO), consistent with the whole-rock MnO content of normal pelitic schists ($X_{Mn} = 0.01–0.04$) (Ferry, 1982; Grambling, 1986).

Except for the loss of volatiles and the movement of certain trace elements, the contact metamorphism of pelitic rocks has been traditionally regarded as an isochemical process (Yardley, 1977). However, the contact metamorphism connected with granitoid intrusives may be accompanied by metasomatism due to high fluid content of silicic melts (Reverdatto et al., 1974; Barton et al., 1991). In order to evaluate the role of metasomatism in this contact aureole, the authors carried out a geochemical study of the country and contact metamorphic rocks, based on com-

Table 1
Whole-rock major element data for country rocks and hornfelses

	Country rocks ($n = 17$)		Hornfelses ($n = 18$)		Cld + Bt zones ($n = 5$)		Grt + And zones ($n = 6$)	
	$\bar{X}$	σ	$\bar{X}$	σ	$\bar{X}$	σ	$\bar{X}$	σ
SiO_2	58.49	0.68	59.59	0.72	59.32	0.46	59.11	0.32
TiO_2	1.02	0.09	1.09	0.07	1.03	0.04	1.05	0.04
Al_2O_3	19.40	0.32	19.76	0.29	19.52	0.18	19.44	0.26
Fe_2O_3	10.12	0.57	10.13	0.44	10.17	0.33	10.28	0.29
MnO	0.24	0.02	0.36	0.06	0.35	0.05	0.36	0.07
MgO	2.05	0.15	2.04	0.19	2.02	0.16	2.05	0.17
CaO	0.58	0.15	0.52	0.11	0.49	0.08	0.51	0.09
Na_2O	1.23	0.11	1.23	0.13	1.22	0.09	1.21	0.07
K_2O	2.82	0.15	2.95	0.18	2.97	0.13	2.99	0.14
P_2O_5	0.09	0.04	0.08	0.05	0.07	0.04	0.06	0.03
L.O.I.	3.85	0.47	2.15	0.51	2.46	0.18	2.34	0.25
Total	99.89		99.90		99.62		99.40	

$\bar{X}$ and σ—component mean value and standard deviation, n—number of analyses. The data are given in wt.% and total iron is expressed as Fe_2O_3. L.O.I.—loss of ignition.

parison of the mean values and dispersion of the whole-rock major elements between hornfelses and unaltered schists (Table 1) using Student's *t*-test and Fisher's *F*-test, according to the methods described by Urbakh (1964). These data reveal that hornfelses and country rocks have identical composition (overlap within errors) for all elements except Mn (Likhanov et al., 1999). A slight increase in Mn content coincides with the transition from country rocks to the chloritoid zone. This is clearly reflected in the relatively high-Mn contents of some rock-forming minerals in the aureole of the Ayakhtinsk granite massif which will be described in more detail later. The difference in MnO content between hornfelses and country rocks may be interpreted by some heterogeneity inherited from the initial protolith. However, some regional metamorphic phylittes collected and described from the study area contain up to 0.35 wt.% MnO (Kozlov, 1994). Relatively high-Mn bulk compositions of these rocks derive from modally abundant and relatively manganiferous chlorites (up to 1 wt.% MnO). In this case, with the exception of loss of ignition (LOI), there are no obvious differences in whole-rock chemical composition between hornfelses and country rocks. In order to evaluate the possibility that the isograds resulted from changes in whole-rock MnO, compositions of hornfelses from group of adjacent zones (chloritoid + biotite vs. garnet + andalusite) were compared in detail. Analytical results (Table 1) show that there are no differences in MnO between the different zones.

5. Mineral chemistry and mineral reactions

For the study area, eight polished sections of rock samples whose bulk compositions were analysed, were prepared for microprobe work. These sample locations are shown by numbers in Fig. 1. Chemical analyses of all mineral phases in the metapelites were obtained using the Camebax electron microprobe analyser in the Institute of Mineralogy and Petrography, Novosibirsk. Operating parameters were 40 nA beam current, 20 kV accelerating voltage, 20 s counting time for all elements and electron beam diameter of 3–4 μm. PAP correction was applied to the data. Natural and synthetic silicate and oxide standards were used for calibration. Representative analyses selected from a larger suite of samples are given in Table 2. Compositions reported here are single spot analyses (not averages). As a check on zonality, all minerals were analysed at the rims and in the core on each grain. For garnet, a regularly spaced traverse across one or two grains per thin section was made. The garnet core and intermediate-zone analyses, with one exception for Samples 25 and 32, are not given here, since they were not used for the pressure and temperature estimates. Presence of graphite and nearly pure ilmenite in every rock indicates that the oxidation potential was low and Fe^{3+} should be minor (Holdaway et al., 1988). The charge balance does not indicate Fe^{3+} in the structural formulas of chlorite, biotite, chloritoid and garnet. Consistent with the assumption of low Fe^{3+}, mineral stoichiometries were determined by normalizing to the indicated number of oxygens: cordierite—18 oxygens, chlorite—14 oxygens, garnet—12 oxygens, micas—11 oxygens, plagioclase and alkali feldspar—8 oxygens, andalusite and sillimanite—5 oxygens, ilmenite—3 oxygens and rutile —2 oxygens.

Because isochemical suites of the pelitic rocks are available, the reactions that occurred can be identified. Equations were calculated among minerals using the actual composition of coexisting minerals by means of the algebraic mass-balance techniques of the program Mathematica, using the built-in function, Nullspace (Likhanov et al., 1994, 1995) for the systems $K_2O–FeO–MgO–Al_2O_3–SiO_2–H_2O \pm MnO \pm TiO_2$ (KFMSAH ± Mn ± Ti). To apply this technique, we constructed a composite matrix for each sample containing (n) number of columns equal to the number of mineral phases in the assemblages and ($n-1$) rows corresponding to the chemical components. H_2O was included as a component in the mass balance. The composition matrix expressed in terms of cations per unit formula. For mass-balance calculations, the water contents in minerals were assumed to be stoichiometric in the model formulae inferred from the widely accepted ones in the literature; the assumption has been made that cordierite contains 0.5 mol of structurally bound water (Bird and Fawcett, 1973; Droop and Treloar, 1981). Chemical reactions were based on the detailed

mineral chemistry and visual modal changes with microtextural observations in the hornfelses.

Prograde chlorite is ubiquitous in the country rocks but abruptly declines in quantity at the cordierite-in isograd and disappears completely within the upper cordierite zone. It is relatively aluminous (up to 3.129) and manganiferous (up to 0.052) as compared with the average chlorite compo-

Table 2
Representative mineral analyses and structural formulae. $X_{Na} = Na/(Na + Ca + K)$, $X_{An} = Ca/(Ca + Na + K)$; for garnets: $X_i = i/T$, where i = Fe, Mg, Mn, Ca and $T = Fe + Mg + Mn + Ca$, for the others minerals: $X_{Fe} = Fe/(Fe + Mg)$. Total Fe expressed as FeO. 0—below detection limit. *N*—sample number

	Muscovite							
Zone	Country rock	Cld	Bt	Grt	And	Lower Crd	Upper Crd	Sil–Kfs
N	12	18	20	25	26	28	32	36
SiO_2	49.54	47.68	47.92	47.83	48.34	46.75	46.31	46.30
TiO_2	0.10	0.20	0.21	0.18	0.04	0.24	0.37	0.61
Al_2O_3	35.30	37.09	36.59	36.18	36.39	36.38	35.67	36.03
FeO	1.58	0.81	0.80	0.78	0.75	0.71	0.76	1.02
MnO	0.02	0	0	0	0.55	0	0	0.01
MgO	0.05	0.35	0.40	0.41	0.41	0.40	0.41	0.37
CaO	0.02	0.03	0.03	0	0	0	0.04	0.03
Na_2O	0.84	1.27	1.29	1.45	1.07	1.01	0.74	0.59
K_2O	7.43	7.98	8.14	7.38	8.47	9.74	9.68	9.54
Total	94.88	95.40	95.38	94.21	96.02	95.23	93.98	93.89
	11(O)							
Si	3.231	3.108	3.140	3.145	3.142	3.087	3.098	3.098
Ti	0.005	0.010	0.010	0.009	0.002	0.012	0.019	0.030
Al	2.714	2.849	2.829	2.805	2.788	2.832	2.812	2.841
Fe	0.086	0.044	0.044	0.043	0.041	0.039	0.043	0.057
Mn	0.001	0	0	0	0.030	0	0	0
Mg	0.005	0.034	0.039	0.040	0.040	0.039	0.041	0.037
Ca	0.002	0.002	0.002	0	0	0	0.003	0.002
Na	0.106	0.160	0.164	0.185	0.135	0.129	0.096	0.077
K	0.618	0.663	0.680	0.618	0.702	0.821	0.826	0.814
X_{Na}	0.146	0.194	0.194	0.230	0.161	0.136	0.104	0.086
	Plagioclase							
Zone	Country rock	Cld	Bt	Grt	And	Lower Crd	Upper Crd	Sil–Kfs
N	12	18	20	25	26	28	32	36
SiO_2	68.54	66.42	65.73	65.52	65.23	64.13	60.59	57.17
Al_2O_3	19.01	21.45	21.80	22.01	22.27	22.81	24.73	26.49
FeO	0	0.20	0.09	0.07	0.06	0.06	0.21	0.17
CaO	0.18	1.52	2.01	2.63	3.01	3.83	6.41	8.72
Na_2O	11.97	10.51	10.34	10.27	10.19	9.35	8.03	7.04
K_2O	0.10	0.08	0.09	0.10	0.11	0.16	0.18	0.16
Total	100.00	100.18	100.06	100.60	100.87	100.34	100.15	99.75
	8(O)							
Si	3.010	2.910	2.883	2.866	2.850	2.820	2.696	2.576
Al	0.980	1.110	1.128	1.135	1.150	1.180	1.297	1.407
Fe	0	0.006	0.003	0.003	0.001	0.001	0.008	0.006
Ca	0.010	0.070	0.096	0.125	0.140	0.180	0.306	0.421
Na	1.020	0.890	0.896	0.863	0.860	0.800	0.693	0.615
K	0.005	0.004	0.005	0.005	0.006	0.009	0.010	0.009
X_{An}	0.010	0.073	0.096	0.125	0.139	0.182	0.303	0.403

(continued on next page)

Table 2 (*continued*)

	Biotite						Chloritoid			
Zone	Bt	Grt	And	Lower Crd	Upper Crd	Sil–Kfs	Cld	Bt	Grt	And
N	20	25	26	28	32	36	18	20	25	26
SiO_2	34.52	34.67	34.74	34.32	34.12	34.03	24.37	24.31	24.32	24.30
TiO_2	1.60	1.62	1.61	1.67	1.53	2.37	0.01	0.02	0.01	0.01
Al_2O_3	19.48	19.33	19.45	20.14	20.62	19.87	39.77	39.82	39.81	39.88
FeO	25.07	25.41	23.85	25.12	25.67	25.95	25.53	25.11	25.17	25.16
MnO	0.16	0.10	0.07	0.18	0.25	0.11	1.30	1.24	1.25	1.27
MgO	6.24	5.83	6.88	5.47	5.05	4.76	1.36	1.53	1.56	1.49
CaO	0.01	0.01	0.01	0.01	0.01	0.02	0.01	0.01	0.01	0.02
Na_2O	0.15	0.16	0.16	0.18	0.23	0.17	0.02	0.01	0.01	0.02
K_2O	8.27	9.40	8.64	8.94	7.97	9.03	0.02	0.02	0.02	0.04
Total	95.50	96.53	95.40	96.03	95.44	96.31	92.38	92.07	92.16	92.19
	11(O)						12(O)			
Si	2.679	2.683	2.687	2.660	2.652	2.644	2.037	2.034	2.033	2.032
Ti	0.093	0.094	0.094	0.097	0.089	0.138	0	0.001	0.001	0.001
Al	1.782	1.763	1.773	1.840	1.889	1.819	3.917	3.927	3.924	3.930
Fe	1.627	1.644	1.543	1.628	1.669	1.686	1.784	1.757	1.760	1.759
Mn	0.011	0.007	0.004	0.012	0.016	0.007	0.092	0.088	0.088	0.090
Mg	0.722	0.672	0.793	0.631	0.585	0.551	0.169	0.191	0.194	0.186
Ca	0.001	0.001	0.001	0.001	0.001	0.002	0.001	0.001	0.001	0.002
Na	0.022	0.024	0.024	0.028	0.034	0.025	0.003	0.002	0.002	0.002
K	0.819	0.928	0.852	0.880	0.790	0.895	0.002	0.002	0.002	0.004
X_{Fe}	0.693	0.710	0.661	0.721	0.740	0.754	0.913	0.902	0.901	0.904

	Chlorite							Cordierite		
Zone	Country rock	Cld	Bt	Grt	And	Lower Crd	Upper Crd	Lower Crd	Upper Crd	Sil–Kfs
N	12	18	20	25	26	28	32	28	32	36
SiO_2	22.32	23.00	22.73	22.78	22.45	22.52	22.94	47.24	47.08	47.60
TiO_2	0.03	0.06	0.05	0.05	0.07	0.05	0.05	0.02	0.03	0.01
Al_2O_3	23.80	23.14	23.31	22.98	22.75	22.48	22.98	32.01	31.70	32.13
FeO	36.44	34.96	34.82	34.61	34.74	31.66	32.27	13.24	13.45	13.16
MnO	0.12	0.55	0.38	0.41	0.55	0.39	0.31	0.43	0.44	0.43
MgO	5.39	6.12	6.72	7.01	7.05	9.22	8.83	4.92	4.91	4.93
CaO	0.04	0.03	0.02	0.02	0.04	0.04	0.03	0.03	0.03	0.04
Na_2O	0.07	0.08	0.05	0.06	0.07	0.04	0.05	0.25	0.29	0.24
K_2O	0.04	0.01	0.01	0.01	0.01	0.01	0.01	0	0	0
Total	88.25	87.95	87.99	87.93	87.72	86.41	87.48	98.14	97.93	98.54
	14(O)							18(O)		
Si	2.490	2.557	2.520	2.529	2.507	2.510	2.527	5.000	5.000	5.010
Ti	0.003	0.005	0.004	0.004	0.006	0.004	0.005	0.001	0.002	0.001
Al	3.129	3.032	3.046	3.007	2.994	2.953	2.983	3.992	3.967	3.986
Fe	3.399	3.250	3.228	3.214	3.244	2.961	2.973	1.170	1.194	1.158
Mn	0.011	0.052	0.036	0.039	0.052	0.037	0.029	0.040	0.040	0.038
Mg	0.896	1.014	1.110	1.160	1.173	1.537	1.449	0.775	0.777	0.773
Ca	0.005	0.004	0.003	0.003	0.004	0.005	0.003	0.006	0.003	0.005
Na	0.015	0.016	0.011	0.013	0.015	0.008	0.011	0.050	0.060	0.049
K	0.005	0.001	0.001	0.001	0.002	0.001	0.001	0	0	0
X_{Fe}	0.791	0.762	0.744	0.735	0.734	0.658	0.672	0.601	0.606	0.600

Table 2 (*continued*)

	Garnet						Andalusite			Sil
Zone	Grt		And	Lower Crd	Upper Crd		And	Upper Crd	Sil–Kfs	Sil–Kfs
N	25 core	25 rim	26 rim	28 rim	32 core	32 rim	26	32	36	36
SiO_2	36.12	36.09	36.08	36.10	36.43	36.26	37.20	37.12	37.05	36.82
TiO_2	0.01	0.03	0.05	0.01	0.15	0.02	0	0.02	0.04	0.02
Al_2O_3	20.31	20.03	20.05	19.99	20.44	20.35	62.03	62.62	61.81	61.92
FeO	26.84	28.50	28.52	31.22	16.75	31.53	0.29	0.34	0.38	0.40
MnO	13.72	12.46	12.48	10.62	22.96	8.03	0	0	0	0.01
MgO	0.60	0.80	0.82	1.21	0.46	1.25	0.03	0.02	0.02	0.01
CaO	1.42	1.15	1.16	0.83	2.70	1.79	0	0.01	0.01	0
Na_2O	0.05	0.06	0.08	0.07	0.04	0.02	0	0.01	0.02	0
K_2O	0	0.01	0.03	0.02	0	0	0	0	0	0
Total	99.07	99.13	99.27	100.07	99.93	99.25	99.55	100.14	99.33	99.18
	12(O)						5(O)			5(O)
Si	2.995	2.989	2.988	2.972	9.987	2.988	1.009	1.002	1.008	1.003
Ti	0.001	0.002	0.003	0.001	0.009	0.001	0	0	0.001	0
Al	1.985	1.952	1.957	1.939	1.975	1.976	1.983	1.991	1.982	1.988
Fe	1.862	1.976	1.978	2.154	1.149	2.175	0.007	0.008	0.009	0.009
Mn	0.963	0.872	0.875	0.740	1.594	0.560	0	0	0	0
Mg	0.074	0.098	0.101	0.148	0.056	0.153	0.001	0.001	0.001	0
Ca	0.126	0.089	0.103	0.073	0.237	0.158	0	0	0	0
Na	0.008	0.009	0.013	0.011	0.006	0.003	0	0.001	0.001	0
K	0	0.001	0.002	0.001	0	0	0	0	0	0
X_{Fe}	0.616	0.651	0.647	0.691	0.378	0.708				
X_{Mn}	0.318	0.287	0.286	0.238	0.525	0.184				
X_{Mg}	0.024	0.032	0.033	0.047	0.018	0.050				
X_{Ca}	0.042	0.021	0.034	0.023	0.078	0.052				

	Rutile	Ilmenite			Alkali feldspar
Zone	Country rock	Cld	Bt	And	Sil–Kfs
N	12	18	20	26	36
SiO_2	0.20	0.01	0.01	0.03	64.97
TiO_2	98.88	53.84	53.16	54.25	0.32
Al_2O_3	0.12	0	0	0.05	18.32
FeO	0.54	44.68	45.01	42.98	0
MnO	0.03	1.18	1.23	1.62	0
MgO	0	0.02	0.01	0.07	0
CaO	0	0.01	0.01	0.02	0
Na_2O	0	0.01	0	0.06	0.80
K_2O	0	0	0	0	15.34
Total	99.77	99.75	99.43	99.08	99.7
	2(O)	3(O)			8(O)
Si	0.003	0	0	0.001	2.998
Ti	0.993	1.017	1.010	1.026	0.011
Al	0.002	0	0	0.001	0.996
Fe	0.006	0.939	0.951	0.905	0
Mn	0	0.025	0.026	0.035	0
Mg	0	0.001	0	0.003	0
Ca	0	0	0	0.001	0
Na	0	0.001	0	0.003	0.072
K	0	0	0	0	0.903

sitions of the low- and medium-pressure pelites in which Al content (2.62) and Mn content (0.04), respectively (Kepezhinskas, 1977). Its Fe/(Fe + Mg) ratio decreases slightly with increasing metamorphic grade from 0.79 in the country rocks to 0.66–0.67 in the lower cordierite zone (Table 2). The Al content of chlorite decreases from 3.129 to 2.95 going from regional grade rocks to the lower cordierite zone. The Si content of chlorite increases from 2.49 in the country rocks to 2.557 in the hornfelses. The pattern of total divalent cations (Ca + Mg + Mn + Ca) variation (from 4.31 in the country rocks to 4.54 in the hornfelses) generally follows the Si pattern, which suggest that Tschermak exchange is the dominant substituational reaction in the chlorite. Retrograde chlorite has the same composition as the prograde variety.

Muscovite, widespread in the country and contact metamorphic rocks, disappears in the sillimanite–alkali feldspar zone. The muscovite-consuming reaction at the sillimanite–alkali feldspar-in isograd in the model KSAH system is

$$0.493\mathrm{Ms} + 0.289\mathrm{Qtz} = 0.482\mathrm{Sil} + 0.445\mathrm{Kfs} + 0.493\mathrm{H_2O}. \quad (1)$$

Muscovite forms a solid solution toward paragonite with a minor amount of celadonite content, expressed as $(\mathrm{Mg} + \mathrm{Fe})/(\mathrm{Mg} + \mathrm{Fe} + \mathrm{Al^{VI}})$ which ranges from 0.08 in the country rocks to 0.04 in the hornfelses. An abrupt increase in paragonite content of muscovite (X_{Na}) from 0.15 to 0.19 coincides with the transition from country rocks to the chloritoid zone (Table 2). Above the biotite zone, X_{Na} continues to increase up to 0.23 at the garnet-in isograd. A distinct decrease in X_{Na} occurs with temperature from 0.16 in the andalusite zone, through 0.14–0.10 in the lower cordierite and upper cordierite zones, respectively, to 0.09 in the sillimanite–alkali feldspar zone. This effect of grade on composition of muscovite is very subtle and approximately the same as those noted by Guidotti (1984) for muscovite from the Rangeley area, ME. Briefly summarized, paragonite content first increases and then decreases as metamorphic grade rises. Decrease in paragonite content as temperature increases in this case is the result of the possible model metamorphic reaction: $\mathrm{Ms_{Na}} + \mathrm{Qtz} = \mathrm{Ms_{K-Na}} + \mathrm{And} + \mathrm{Pl} + \mathrm{H_2O}$ (Korikovskii, 1979), where the muscovite of the left hand side of this reaction is more Na-rich than the muscovite on the right hand side.

Plagioclase in the country rocks is essentially homogeneous albite with anorthite content (X_{An}) of 0.01. The plagioclase of the chloritoid, biotite and garnet zones is slightly more calcic, in the range $X_{\mathrm{An}} = 0.073–0.125$. The X_{An} of oligoclase increases in the andalusite zone up to 0.139 and at the cordierite-in isograd X_{An} is 0.182. An abrupt change in plagioclase composition to sodic andesine ($X_{\mathrm{An}} = 0.303–0.403$) coincides with the garnet-chlorite-out and sillimanite–alkali feldspar-in isograds of the upper cordierite and sillimanite–alkali feldspar zones of contact aureole, respectively (Table 2).

Chloritoid, one of the most abundant minerals of the chloritoid, biotite and garnet zone, disappears within the andalusite zone. The mineral is chemically homogeneous and remarkably iron-rich with Fe/(Fe + Mg) in the narrow range 0.90–0.91. MnO content is relatively high and varies only slightly (1.25–1.30 wt.%). Chloritoid as a stable phase is not abundant and rare in typical contact aureoles due to a narrow temperature interval at low pressure of contact metamorphism (Ganguly, 1969; Hoschek, 1969; Kolobov et al., 1992). If chloritoid occurs, it is found only in rocks of Fe-aluminous bulk composition that plot on the high-Al side of the critical Grt–Chl join in the AFM-projection (Albee, 1972; Harte, 1975). This is consistent with the Al-rich bulk composition of the studied hornfelses ($X_{\mathrm{Al}} = 0.30–0.32$). The possible chloritoid-forming reaction at the chloritoid-in isograd in the KFMASHTi system is

$$0.704\mathrm{Ms_{c.r}} + 0.023\mathrm{Chl} + 0.065\mathrm{Rt} = 0.657\mathrm{Ms_{c.z}} + 0.029\mathrm{Cld} + 0.061\mathrm{Ilm} + 0.237\mathrm{Qtz} + 0.084\mathrm{H_2O}, \quad (2)$$

where $\mathrm{Ms_{c.r}}$ and $\mathrm{Ms_{c.z}}$ are the muscovites from country rocks and chloritoid zone, respectively. This reaction appears on the AKF diagram (Fig. 5) as the intersection of the $\mathrm{Ms_{c.r}}$–Chl with $\mathrm{Ms_{c.z}}$–Cld tie-line. Evidence for reaction comes from the observed replacement of muscovite–chlorite aggregates by chloritoid as well as rutile by ilmenite. The chloritoid isograd has been discussed by Chinner (1967), who proposed pyrophyllite-, kaolinite- and paragonite-breakdown reactions to explain it. However, XRD examination (Kozlov, 1994) has shown the absence of these phases in the low-grade equivalents of the

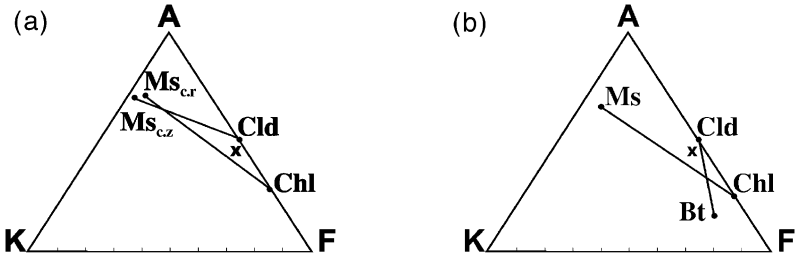

Fig. 5. AKF diagram showing composition of whole rocks (x) and minerals (dots) at the chloritoid-in (a) and biotite-in (b) isograds. Tie-lines joining $Ms_{c.r}$–Chl and $Ms_{c.z}$–Cld (a), Ms–Chl and Cld–Bt (b) are shown as solid lines. A = Al_2O_3–K_2O–Na_2O; F = FeO + MgO + MnO; K = K_2O (in molecular percentages). c.r—country rocks, c.z—chloritoid zone.

chloritoid-bearing pelites. Thus, chloritoid has clearly grown at the expense of relatively aluminous chlorite, perhaps by an equilibrium such as reaction (2). This is in accordance with the chloritoid-forming reactions proposed by Thompson and Norton (1968) and Frey (1978).

Ilmenite, the dominant oxide mineral, typically appears at the chloritoid-in isograd and occurs in all metamorphic grades. Its Mn content is in the narrow range (0.025–0.035). Rutile has a more restricted occurrence than ilmenite and is present only in the country rocks.

Biotite appears in the biotite zone and occurs in all of the contact metamorphic zones. The tetrahedral Al, Ti content (from 0.093 to 0.138) and Fe/(Fe + Mg) ratio (from 0.69 in the biotite zone to 0.75 in the sillimanite–alkali feldspar zone) increase slightly with increasing metamorphism grade. Its Mn content varies slightly (0.04–0.016). Wang and Spear (1991) discussed the coexistence of chloritoid + biotite in the Walloomsac Formation north of Dutchess Country, and proposed that occurrence of this assemblage was largely controlled by the bulk composition of the rock. Chloritoid and biotite are predicted to coexist if bulk Fe/(Fe + Mg + Mn) > 0.60. This is consistent with the bulk composition of the hornfelses studied. The mineral reaction responsible for the first appearance of biotite at the biotite-in isograd in the KFMASH system is

$$0.439\mathrm{Ms} + 0.285\mathrm{Chl} + 0.322\mathrm{Ilm} = 0.372\mathrm{Cld} + 0.364\mathrm{Bt} + 0.359\mathrm{Qtz} + 0.472\mathrm{H_2O}. \quad (3)$$

This reaction appears on the AKF diagram (Fig. 5) as the intersection of the muscovite–chlorite with chloritoid–biotite tie-line. The reaction is confirmed by mineral abundances in thin section, where the formation of biotite and chloritoid is accompanied by decreasing amounts of chlorite and muscovite. The observed chemographic relations (Fe/(Fe + Mg): Bt < Chl < Cld) at the biotite-in isograd are also consistent with the calculated reaction (Fig. 2). This reaction is important because it signifies the lower thermal stability limit for the chloritoid + biotite mineral assemblage.

Garnet-bearing assemblages occur sporadically within the garnet, andalusite and lower cordierite zones. There are no significant differences in garnet composition between different zones. Garnets are $(Fe,Mg,Mn,Ca)_3Al_2Si_3O_{12}$ solid solutions. They exhibit normal growth zoning, with grossular and spessartine components decreasing and almandine and pyrope components increasing from core to rim. Core compositions are Sps_{32} $Alm_{62}Grs_{04}Prp_{02}$ and rim compositions are $Alm_{66}Sps_{29}Prp_{03}Grs_{02}$ (Table 2). The first appearance of garnet in the pelitic rocks near the andalusite-in isograd was probably the result of the following model reaction at the garnet-in isograd in the KFMASH system

$$0.207\mathrm{Bt} + 0.368\mathrm{Cld} + 0.800\mathrm{Qtz} = 0.250\mathrm{Grt} + 0.311\mathrm{Ms} + 0.149\mathrm{Chl} + 0.035\mathrm{H_2O}. \quad (4)$$

On the AFM diagram (Fig. 2), this mineral reaction appears as the crossed tie-lines of the biotite–chloritoid and garnet–chlorite within the Fe, Mg-end-member system and is responsible for the paragenesis garnet + chlorite in the KFMASH sys-

tem. The small amount of MnO present in most metapelites is sufficient to stabilize garnet in many assemblages (e.g. Symmes and Ferry, 1992). Evidence supporting the proposed balanced garnet-forming reaction is confirmed by the uniformity of bulk-rock compositions with respect to all components (particularly MnO) across the garnet-in isograd. If the system is isochemical, then some Mn must have been supplied to the garnet from the most abundant and relatively high-Mn chloritoid of the biotite zone as a possible reactant for garnet formation. The presence of chloritoid inclusions in garnet may be textural evidence for this reaction. The chloritoid modal abundance (up to 25%) at the garnet-in isograd is significantly higher than the garnet one (up to 3%). Spear and Cheney (1989) calculated that Fe–Mg garnet should not be stable in low-grade metapelites except for very Fe-rich bulk compositions. This is consistent with the bulk composition of these hornfelses. This reaction has been described by Whitney et al. (1996) for pelitic schists in Dutchess County where it does occur at about the same grade as the garnet-in isograd in hornfelses studied. In this low-grade sequence, the first appearance of garnet at the expense of chloritoid + biotite was not a function of the bulk composition of the protolith.

Garnet and chlorite disappear simultaneously in the lower cordierite zone owing to the following reaction at the garnet- and chlorite-out isograd in the KFMASH system

$$0.204\mathrm{Ms} + 0.246\mathrm{Chl} + 0.075\mathrm{Grt} + 0.471\mathrm{Qtz} = 0.422\mathrm{Bt} + 0.166\mathrm{Crd} + 0.682\mathrm{H_2O}. \quad (5)$$

This reaction marks the upper stability of chlorite + garnet in muscovite-bearing rocks, so that above this reaction chlorite and garnet no longer appears on the AFM diagram (Fig. 2). All the rocks above garnet-out isograd contain biotite and cordierite as principal minerals. The destruction of garnet and chlorite must have involved some combination of these minerals. This reaction is consistent with the observed chemographic relations ($Fe/(Fe + Mg)$: Crd < Chl < Bt < Grt) at the garnet- and chlorite-out isograd (Fig. 2).

The compositions of andalusite and sillimanite in the aureole are close to end member Al_2SiO_5. With increasing metamorphic grade, andalusite modal abundance and grain size generally increase. The following KFMASH (6) and KFMASHTi (7) reactions mark the first appearance of andalusite in hornfelses for garnet-bearing assemblages

$$0.329\mathrm{Ms} + 0.180\mathrm{Chl} = 0.272\mathrm{Bt} + 0.089\mathrm{Grt} + 0.404\mathrm{And} + 0.082\mathrm{Qtz} + 0.779\mathrm{H_2O}, \quad (6)$$

and for ilmenite- and chloritoid-bearing assemblages

$$0.399\mathrm{Ms} + 0.236\mathrm{Chl} + 0.028\mathrm{Ilm} = 0.329\mathrm{Bt} + 0.169\mathrm{Cld} + 0.289\mathrm{And} + 0.328\mathrm{Qtz} + 0.676\mathrm{H_2O}. \quad (7)$$

Fig. 2 provides an explanation for these reactions. Reaction (7) may account for the formation of the rare mineral assemblage andalusite + biotite + chloritoid. Based on the numerous observed mineral assemblages in contact metamorphosed pelites, the assemblage garnet + chlorite + andalusite + muscovite is considered to be unstable in pure KFMASH system (Pattison and Tracy, 1991). The strong partitioning of MnO into garnet expands the stability field of garnet-bearing assemblages (Spear, 1993). It is well established that the incorporation of Mn into ferromagnesian silicate minerals can modify phase relations by shifting KFMASH equilibria in $P–T$ space and allowing incompatible KFMASH mineral assemblages to exist under the same $P–T$ conditions in compositions with different Mn contents (e.g. Symmes and Ferry, 1992; Droop and Harte, 1995). In order to evaluate the effect of Mn on the possible mass-balance relations at the formation of andalusite, all manganiferous phases (ilmenite, chloritoid, chlorite and garnet) have been involved in the calculations. The overall andalusite-forming reaction may be written in the KFMASHTiMn system as

$$0.395\mathrm{Ms} + 0.231\mathrm{Chl} + 0.028\mathrm{Ilm} = 0.325\mathrm{Bt} + 0.303\mathrm{And} + 0.151\mathrm{Cld} + 0.011\mathrm{Grt} + 0.3\mathrm{Qtz} + 0.693\mathrm{H_2O}. \quad (8)$$

Thus, the addition of Mn component to a KFMASH system does not change significantly the behaviour of the reactions (6) and (7).

Cordierite is the most abundant and widespread ferromagnesian phase within the cordierite and alkali feldspar zones of the aureole. Cordierite is chemically homogeneous with constant $Fe/(Fe + Mg)$ in the narrow range 0.60–0.61. Its Mn content is in the

narrow range (0.038–0.04). The following KFMASH (Eqs. (9) and (10)) reactions mark the first appearance of cordierite at the cordierite-in isograd for garnet-bearing assemblages

$$0.263\mathrm{Ms} + 0.213\mathrm{Chl} + 0.018\mathrm{Grt} + 0.452\mathrm{Qtz} = 0.245\mathrm{Bt} + 0.240\mathrm{Crd} + 0.75\mathrm{H_2O}, \quad (9)$$

and for garnet- and andalusite-bearing assemblages

$$0.403\mathrm{Ms} + 0.164\mathrm{Chl} + 0.083\mathrm{Grt} = 0.376\mathrm{Bt} + 0.053\mathrm{Crd} + 0.442\mathrm{And} + 0.190\mathrm{Qtz} + 0.654\mathrm{H_2O}. \quad (10)$$

The reactions are consistent with the observed chemographic relations ($Fe/(Fe + Mg)$: Crd < Chl < Bt < Grt) at the cordierite-in isograd and supported by mineral abundances in thin section, where the appearance of cordierite + biotite is accompanied by decrease in modal amounts of chlorite, muscovite and garnet. Cordierite increases in modal amount up to the sillimanite–alkali feldspar zone. Cordierite + garnet + muscovite is a rare assemblage in low-pressure contact metamorphic rocks, having been noted only in five contact aureoles; it has also been reported in several medium-grade regional metamorphic settings (Pattison and Tracy, 1991), showing no consistent relationship with grade and pressure. Thus, the appearance and stability of this rare mineral assemblage as well as the discussed above garnet + andalusite + chlorite + muscovite discussed above assemblage are connected with Mn-enriched garnet composition and whole-rock composition rather than P–T conditions.

The first development of sillimanite coincides closely with local reaction (1) the Ms + Qtz breakdown. In most rocks, the sillimanite occurs adjacent to cordierite poikiloblasts and alkali feldspar in a matrix of quartz, muscovite, ilmenite, plagioclase and locally biotite. This suggests that sillimanite formed from the reaction of matrix minerals in which it nucleated as is suggested for the Ballachulish aureole in Scotland (Pattison, 1992) and for the sillimanite-bearing pelites near Rangeley in USA (Foster, 1977). As noted by Pattison (1992), these observations carry significant implications for the interpretation of andalusite/sillimanite relations in other low-pressure settings. This study therefore contrasts with Kerrick and Woodsworth (1989), who argued that the equilibrium boundary between andalusite and sillimanite is where andalusite is replaced by sillimanite, and that lower-grade occurrences of sillimanite in andalusite-bearing rocks represented metastable growth in the andalusite field. Taking into account that sillimanite must have formed by reactions involving matrix minerals, it is possible to write the sillimanite-forming reaction at the sillimanite–alkali feldspar-in isograd in KFMASH system as

$$0.494\mathrm{Ms} + 0.002\mathrm{Bt} + 0.362\mathrm{Qtz} = 0.024\mathrm{Crd} + 0.435\mathrm{Sil} + 0.448\mathrm{Kfs} + 0.483\mathrm{H_2O}. \quad (11)$$

The alkali feldspar in the hornfelses of the inner zone is microcline with a fairly narrow bulk compositional range around Or_{93}.

6. Thermodynamic conditions of contact metamorphism

Metamorphic conditions for contact metamorphism in the Ayakhtinsk aureole were deduced on the basis of (1) independent pressure estimates obtained from net-transfer equilibria in metapelites and projections of albite–orthoclase–quartz components of granitoid into haplogranite system of Tuttle and Bowen (1958), (2) estimates of metamorphic temperatures obtained from exchange and solvus thermometers, and (3) quantitative petrogenetic grids using the isopleth method (Table 3; Fig. 6). Finally, P and T estimates were compared with dehydration equilibria in order to evaluate fluid-composition models (Table 4). In addition, the conditions of formation of the mineral assemblages outlined above were determined, using microprobe analyses of the minerals and the computer software, THERMOCALC (Powell and Holland, 1988, 1994), with the internally consistent thermodynamic dataset of Holland and Powell (1990) (Table 5; Fig. 6). The activities of end-member components of analysed minerals were calculated using the activity–composition relations suggested by Holland and Powell (1990). The results of these P–T calculations are summarized in Table 5.

Table 3
Pressure and temperature estimates calculated from various geothermobarometers in metapelites

Zone	*N*	T (°C)							*P* (kbar)				
		1	2	3	4	5	6	Mean	7	8	9	10	Mean
Country rock	12	400	400					400					
Cld	18		430										
Bt	20		448	452				450					
Grt	25		480										
And	26		490		510	500		500	2.9	3.1			
Lower Crd	28		553		542	578	560	560	3.2	3.1	2.9		3.2
Upper Crd	32		613			632	620	620	3.5	3.5		3.1	
Sil–Kfs	36		640										

Geothermometers: (1) Ms–Chl (Kotov, 1986), (2) Pl–Ms (Green and Usdansky, 1986b), (3) Bt–Cld (Perchuk, 1991), (4) Bt–Ms (Hoisch, 1989), (5) Crd–Grt and Grt–Bt (Perchuk, 1991), (6) Crd–Grt and Grt–Bt (Thompson, 1976). Geobarometers: (7) Grt–Bt–Ms–Pl (Ghent and Stout, 1981) with modifications by Hodges and Crowley (1985); (8, 9 and 10) Grt–Bt–Ms–Pl, Grt–Bt–Pl and Grt–Ms–Pl (Hoisch, 1990); *N*—sample number.

6.1. Pressure

Several independent estimates of pressure in the Ayakhtinsk Igneous Complex and thermal aureole have been made, all of which show a high degree of consistency. Dazenko (1984) projected CIPW-normative albite–orthoclase–quartz components of granitoid samples from the Ajakhtinsk Igneous Complex into the Ab–Kfs–Qtz ternary of Tuttle and Bowen (1958). The samples plot along the P_{H_2O} = 3–3.5 kbar thermal valley, with late crystallizing leucogranites plotting on, or near, the 3–3.5 kbar thermal minimum. The cotectic, near-minimum compositions of the leucogranites suggest water-excess

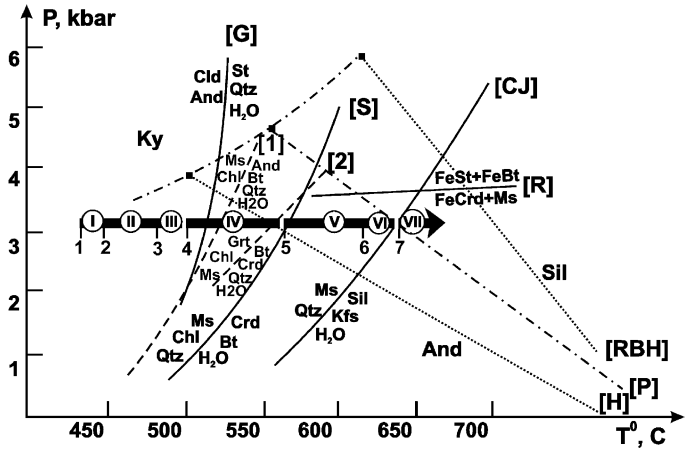

Fig. 6. Schematic *P–T* diagram showing the positions of metamorphic zones and isograds in the Ayakhtinsk intrusion contact aureole and comparison of calculated equilibria [P] (Pattison, 1992) with experimental data [CJ] (Chatterjee and Johannes, 1974), [G] (Ganguly, 1969), [R] (Richardson, 1968) and [S] (Seifert, 1970). The solid square and accompanyng dot-dashed lines are the triple point and And = Sil curve of Pattison (1992). The solid squares and accompanying dotted lines [H] and [RBH] are the triple points and experimental And = Sil curves of Holdaway (1971) and Richardson et al. (1969), respectively. *P–T* locations of the univariant equilibria calculated using the program THERMOCALC are indicated by dashed lines. Roman numerals: contact metamorphic zones referred to in the text. Arabic numerals indicate isograds: (I) Cld-in, (II) Bt-in, (III) Grt-in, (IV) And-in, (V) Crd-in, (VI) Grt–Chl-out and (VII) Sil–Kfs-in. The solid arrow represents the inferred isobaric prograde trajectory in the Ayakhtinsk contact aureole.

Table 4
Summary of water fugacity, activity and mole fraction estimates in the metamorphic fluid

Zone	N	$f^{\circ}_{H_2O}$ (bar)	f_{H_2O} (bar)	a_{H_2O}	X_{H_2O}	
					Model 1	Model 2
Bt	20	874	774	0.89	0.89	0.85
Grt	25	1028	867	0.84	0.85	0.77
And	26	1134	628	0.55	0.56	0.35
Lower Crd	28	1462	900	0.62	0.63	0.46
Sil–Kfs	36	1895	907	0.48	0.49	0.36

Calculated using the following mineral equilibria at estimated T and P: 20–Ms + Chl = 2Cld + Bt + Qtz + $2H_2O$; 25–2Ms + 3Chl = 3Cld + 2Bt + 2Grt + $9H_2O$; 26–5Ms + 3Chl = 5Bt + 8And + Qtz + $12H_2O$; 28–Ms + Chl + 2Qtz = Crd + Bt + $4H_2O$; 36–Ms + Qtz = Sil + Kfs + H_2O. $f^{\circ}_{H_2O}$ and f_{H_2O}—fugacity of pure H_2O and in mixture, respectively, at the T and P of interest; a_{H_2O}—activity of H_2O; X_{H_2O}—mole fraction for H_2O in the metamorphic fluid. Model 1 assumes ideal mixing, model 2 assumes non-ideal mixing of H_2O in the fluid phase. N—sample number.

crystallization at lithostatic pressure near 3–3.5 kbar, corresponding to a depth of 10 ± 1 km, assuming an average rock density of 2.7 g/cm^3, since lower water pressures would shift the cotectic/minimum intersection towards albite-depleted compositions (Johannes, 1985). Four geobarometers involving Grt–Bt–Ms–Pl (Ghent and Stout, 1981) with modifications by Hodges and Crowley (1985) and Hoisch (1990), Grt–Bt–Pl and Grt–Ms–Pl (Hoisch, 1990) were used to determine aureole pressures. Garnet rim compositions, neighbouring biotite, muscovite and plagioclase compositions were used with activity–composition models of Hodges and Crowley (1985) and Hoisch (1990). The fluid pressure derived within the thermal aureole of the igneous complex is $P_{H_2O} = 3.2 \pm 0.3$ kbar (Table 3). The value obtained is similar to the intersection of the pure-phase experimental equilibria Ms + Qtz = Sil + Kfs + H_2O (Chatterjee and Johannes, 1974) and And = Sil curve from Pattison (1992) (Fig. 6). The And = Sil curve and triple point used here lie midway between the determinations of Holdaway (1971) and Richardson et al. (1969), and agree closely with the estimates of Holland and Powell (1990) and Bohlen et al. (1991). Kerrick and Heninger's (1984) data for sillimanite stability are in agreement with the preferred location of And = Sil of this study. For comparison, intersection of the Ms + Qtz = Sil + Kfs + H_2O reaction with the And = Sil curves of Holdaway (1971) and Richardson et al. (1969) give pressures of 2.1 and 4.1 kbar, respectively. Using the calibrated grid of Holdaway and Lee (1977), one obtains a pressure estimate using the isopleth method. Taking the measured Fe/Fe + Mg cordierite value of 0.60 for the univariant assemblage Crd + Kfs + Sil + Bt + Ms + Qtz at the study area, Holdaway and Lee's calibrated grid gives 2.6 kbar for $a_{H_2O} = 1.0$. However, according to Skippen and Gunter (1996) and Carey (1995), the stability of cordierite is enlarged and extended to higher pressure (> 3 kbar) in comparison to the anhydrous phase relations. The presence of Fe-cordierite rather than staurolite also provides an upper pressure constraint. In the end-member Fe-system, cordierite breaks down to staurolite at approximately 3 kbar (Richardson, 1968; Holdaway and Lee, 1977). The maximum possible pressure stability of Fe-cordierite in muscovite-bearing pelites is shown on Fig. 6. In addition, Pattison (1992) noted that And = Sil curve of Holdaway (1971) results in andalusite + biotite + cordierite ± chlorite assemblages being restricted to very low pressures and to very Fe-rich compositions, which seems to contradict the widespread development of these assemblages in nature. Based on a large number of well documented aureoles (Table 2 of Pattison and Tracy, 1991) the Ayakhtinsk aureole belongs to cordierite–andalusite facies series 2a, which corresponds to a pressure range of 3–4 kbar. A pressure of 3.2 kbar with ±1 kbar uncertainties in pressure calculations is in a good agreement with that obtained from other contact aureoles with the mineral assemblages chloritoid + biotite and chloritoid + biotite + andalusite (2.5–3.5 kbar; Okuyama-Kusunose, 1994; Likhanov, 1988b, 1989) and pressure estimates from THERMOCALC average P–T results (Table 5).

6.2. Temperature

Seventeen mineral pairs were analysed in thin section domains in which the two selected minerals were not in physical contact by using inner rims of garnet and matrix mineral compositions. Temperature estimates in the Ayakhtinsk intrusion contact aureole were obtained using geothermometers involving Ms–Chl (Kotov, 1986), Pl–Ms (Green and

Table 5
THERMOCALC results for a muscovite–biotite–chlorite–chloritoid–garnet–andalusite–plagioclase–quartz (Andalusite zone, Sample 26), muscovite–biotite–andalusite–cordierite–garnet –chlorite–quartz–plagioclase (Lower cordierite zone, Sample 28), muscovite–biotite–chlorite–chloritoid–garnet–plagioclase–quartz (Garnet zone, Sample 25), and muscovite–biotite–cordierite–sillimanite–alkali feldspar–plagioclase–quartz (Sillimanite–alkali feldspar zone, Sample 36) mineral assemblages from the Ayakhtinsk contact aureole

Andalusite zone, Sample 26
Activities: mu(0.700), pa(0.700), cel(0.0096), phl(0.0239), ann(0.103), east(0.024), py(5.3e − 5), gr(3.6e − 4), alm(0.230), spss(0.023), clin(0.00104), daph(0.150), ames(0.0029), mctd(0.109), fctd(0.860), mnctd(0.044), ab(0.850), an(0.220), and(1.00), q(1.00), H_2O(1.00,0.35)
Independent set of 12 reactions
Temperature estimates (°C)

	2.5 kbar		3.0 kbar		3.5 kbar	
X_{H_2O}	avT $\pm 2\sigma$	Fit	avT $\pm 2\sigma$	Fit	avT $\pm 2\sigma$	Fit
1.00	530 ± 18	2.0	540 ± 20	2.2	549 ± 22	2.3
0.35	476 ± 20	1.9	486 ± 22	2.0	494 ± 24	2.2

Lower cordierite zone, Sample 28
Activities: mu(0.780), pa(0.810), cel(0.0101), phl(0.0151), ann(0.120), east(0.017), py(0.00016), gr(1.2e − 5), alm(0.270), spss(0.014), clin(0.0036), daph(0.084), ames(0.0081), crd(0.200), fcrd(0.350), mncrd(0.00045), ab(0.810), an(0.290), and(1.00), q(1.00), H_2O(1.00,0.46)
Independent set of 12 reactions
Temperature estimates (°C)

	2.5 kbar		3.0 kbar		3.5 kbar	
X_{H_2O}	avT $\pm 2\sigma$	Fit	avT $\pm 2\sigma$	Fit	avT $\pm 2\sigma$	Fit
1.00	585 ± 26	2.3	597 ± 30	2.7	610 ± 38	3.3
0.46	534 ± 36	3.0	545 ± 44	3.6	554 ± 52	4.4

Garnet zone, Sample 25
Activities: mu(0.690), pa(0.810), cel(0.010), phl(0.0167), ann(0.130), east(0.017), py(4.8e − 5), gr(3.5e − 4), alm(0.240), spss(0.023), clin(0.00108), daph(0.157), ames(0.0027), mctd(0.100), fctd(0.860), mnctd(0.045), ab(0.870), an(0.190), q(1.00), H_2O(1.00,0.77)
Independent set of 11 reactions

X_{H_2O}	Average P–T ($\pm 2\sigma$)		Corr	Fit
1.00	T = 508 ± 38 °C	P = 3.1 ± 2.8 kbar	0.627	1.77
0.77	T = 491 ± 36 °C	P = 3.1 ± 2.6 kbar	0.631	1.73

Sillimanite-alkali feldspar zone, Sample 36
Activities: mu(0.750), pa(0.510), cel(0.0089), phl(0.0096), ann(0.130), east(0.013), crd(0.190), fcrd(0.350), mncrd(0.00044), ab(0.590), an(0.640), sill(1.00), and(1.00), mic(1.00), q(1.00), H_2O(1.00,0.36)
Independent set of 8 reactions

X_{H_2O}	Average P–T ($\pm 2\sigma$)		Corr	Fit
1.00	T = 673 ± 50 °C	P = 3.1 ± 1.2 kbar	0.910	0.61
0.36	T = 638 ± 42 °C	P = 3.6 ± 1.2 kbar	0.884	0.46

Abbreviations for the end-members of the minerals are adopted from Powell and Holland (1998): mu—muscovite, pa—paragonite, cel—celadonite; phl—phlogopite, ann—annite, east—eastonite; ames—amesite, daph—daphnite, clin—clinochlore; mctd—Mg-chloritoid, mnctd—Mn-chloritoid, fctd—Fe-chloritoid; py—pyrope, gr—grossular, alm—almandine, spss—spessartine; crd—cordierite, fcrd—Fe-cordierite, mncrd—Mn-cordierite; ab—albite, an—anorthite; q—quartz; and—andalusite; sill—sillimanite; mic—microcline. Average P–T and T estimates were made at $X_{H_2O} = 1$ and X_{H_2O} calculated assuming non-ideal mixing of water in the fluid phase from Table 4. avT—average temperature.

Usdansky, 1986b), Bt–Cld (Perchuk, 1991), Bt–Ms (Hoisch, 1989), Crd–Grt and Grt–Bt (Perchuk, 1991; Thompson, 1976). For the most part, these calibrations are based on the comparison of natural assemblages with experimental phase equilibria by adopting an ideal cation-mixing model in both the minerals. The empirical calibration of Hoisch (1989) was based on the exchange of Mg-Tschermak's component between muscovite and biotite that models nonideality in the mixing of cations within the octahedral sites of both muscovite and biotite. The Na–K exchange reaction between plagioclase and muscovite has been used utilizing a ternary-feldspar subregular solution model and a non-ideal binary white mica solution model (Green and Usdansky, 1986b). Temperatures generally increase with metamorphic grade as indicated in the average estimate for each zone in Table 3 and are comparable to the temperature estimate obtained from the reactions in Fig. 6. The temperature of the regional metamorphism in the country rocks calculated by the Ms–Chl (Kotov, 1986) and Pl–Ms (Green and Usdansky, 1986b) geothermometers is 400 °C, thus corresponding to the greenschist facies. Temperatures calculated for thermal metamorphism lie within the range 430–640 °C with an error of ± 50 °C and correspond to the muscovite- and amphibole-hornfels facies (Reverdatto, 1973). The temperature of initial contact metamorphism at the chloritoid-in isograd is 430 °C, according to the Ms–Pl geothermometer (Green and Usdansky, 1986b). The average temperature at the biotite-in isograd is 450 °C; this agrees with temperature estimations on the first appearance of biotite in association with chloritoid for rocks of similar composition from the Karatash aureole and with Spear and Cheney's (1989) petrogenetic grid for the KFASH system. Four geothermometers yield average temperature estimates of 480 °C at the garnet-in isograd, 500 °C at the andalusite-in isograd and 560 °C at the cordierite-in isograd, consistent with experimental and calculated data (Hsu, 1968; Fig. 6; Table 5). Using the calibrated grid of Spear and Cheney (1989), one obtains a temperature estimate using the isopleth method of about 3 kbar. Taking the measured Fe/Fe + Mg garnet value of 0.95 and Mn/Mn + Mg + Fe value of 0.2 for the univariant assemblage Ms + Qtz + Bt + Chl + Grt + Cld Spear and Cheney's calibrated grid gives 470 °C for $a_{H_2O} = 1.0$. The data are also consistent with the petrogenetic grid and temperature estimations at the cordierite-in isograd for graphite-bearing metapelites of the Ballachulish aureole (Pattison, 1989; Pattison and Tracy, 1991). An average temperature at the garnet- and chlorite-out isograd is 620 °C. The first appearance of sillimanite with alkali feldspar in the contact aureole took place at $T = 640$ °C. Application of the average P–T approach of Powell and Holland (1988, 1994), using the program THERMOCALC, yielded estimates of $T = 673 \pm 50$ °C at $P = 3.1 \pm 1.2$ kbar and $a_{H_2O} = 1.00$; $T = 638 \pm 42$ °C at $P = 3.6 \pm 1.2$ kbar and $a_{H_2O} = 0.36$ (2σ errors; Table 5) for the sillimanite–alkali feldspar zone.

6.3. Fluid composition

The composition of the fluid phase is an important variable in graphite-bearing pelitic rocks during progressive dehydration because of the development of CH_4, CO_2, H_2 and CO (French, 1966). This lowers P_{H_2O} and affects the stability fields of mineral assemblages (e.g. Holdaway, 1978). Ohmoto and Kerrick (1977) argued that during dehydration reactions in graphitic pelites, the fluid is internally buffered to a composition of maximum H_2O content. At 3 kbar, the maximum proportion of H_2O in a hydrous fluid decreases with increasing temperature from $X_{H_2O} = 0.92$ at $T = 450$ °C to 0.77 at 640 °C, assuming ideal mixing (i.e., $X_{H_2O} = a_{H_2O}$). If non-ideal mixing is assumed, then X_{H_2O} will be somewhat lower because activity coefficients are positive for H_2O in H_2O–CO_2–CH_4 mixtures (Kerrick and Jacobs, 1981). More rigorous arguments presented by Connolly and Cesare (1993) showed that during simple dehydration, graphite-saturated C–O–H fluids are generated with, rather than buffered toward, the maximum thermodynamic activity of H_2O.

Thermodynamic analysis of mineral equilibria with a fluid phase was applied to calculate partial pressures of the gas species using the Gibbs method (treated in detail by Spear et al., 1982). It specifies quantitatively the equilibrium relationships between the pressure, temperature, mineral composition and activity of gas species in a mineral assemblages for which a dehydration equilibrium can be written among phase components. Mathematical expressions and subsequent thermodynamic calculations of fluid

phase composition were made according to the methods described by Ferry (1976).

At fixed P and T, the abundances of all C–O–H components in the fluid may be determined if one variable, such as f_{O_2}, is fixed. Because in the majority of the graphitic pelites in the aureole ilmenite is the only oxide phase present, an independent estimation of f_{O_2} by magnetite–ilmenite or magnetite–graphite oxybarometry is not possible.

Mineral dehydration equilibria calculated for biotite-in, garnet-in, andalusite-in, cordierite-in, sillimanite-in isograds have been used in conjunction with the above estimates of T and P to determine the fugacity of H_2O in the metamorphic fluid phase (Table 4). All phase equilibrium calculations reported here were done with the mineral end-member data of Holland and Powell (1990); mixing properties of mineral solutions were taken for cordierite from Aranovich and Podlesskii (1989), for biotite and muscovite from Hoisch (1991), for garnet from Hodges and Crowley (1985) and for alkali feldspar from Green and Usdansky (1986a); all other mineral solutions from Holland and Powell (1990). The mole fraction of H_2O (X_{H_2O}) in the metamorphic fluid was determined on the basis of two models: (1) ideal mixing of H_2O–CO_2 in the fluid phase and (2) non-ideal mixing of H_2O–CO_2 in the fluid phase based on the subregular solution activity model of Powell and Holland (1985). If ideal mixing in the fluid phase is assumed, an estimate of H_2O mole fraction can be calculated from the fugacity (at known P and T) with the expression: $X_{H_2O} = f_{H_2O}/(\Upsilon_{H_2O} \times P)$, where Υ_{H_2O} is the fugacity coefficient of pure water at the P and T of interest from Duan et al. (1992). The expression for the second model is $X_{H_2O} = a_{H_2O}/\exp[X^2_{CO_2}(W_{H_2O} + 2X_{H_2O}(W_{CO_2} - W_{H_2O})]$, at $X_{H_2O} + X_{CO_2} = 1$ and where W_{H_2O} and W_{CO_2} are the Margules parameters from Powell and Holland (1985).

The X_{H_2O} and a_{H_2O} estimates for the metamorphic fluid decrease toward the intrusive contact from 0.89–0.85 at $T = 450$ °C to 0.49–0.36 at $T = 640$ °C, assuming ideal and non-ideal mixing, respectively, of water in the fluid phase (Table 4). These values are in agreement with the data of Ohmoto and Kerrick (1977) and Connolly and Cesare (1993) on the evolution of C–O–H fluid composition in equilibrium with graphite taking into account the uncertainty of the X_{H_2O} and a_{H_2O} values caused by errors in both temperature and mineral composition (Ferry, 1980). The observed correlation between calculated temperature and X_{H_2O} may be taken as evidence that mineral assemblages in metapelites buffer the composition of metamorphic fluid with which they are in equilibrium. It is concluded that an aqueous fluid varying in composition from the outer to the inner aureole could have been in local equilibrium with the mineral assemblages of the contact aureole. Varying compositions were imposed upon the fluid by the buffering capacity of the mineral assemblages of each bed, proving the concept of the buffering capacity of the mineral assemblages with respect to volatile components, as recognized by James and Howland (1955) and developed by Greenwood (1975).

7. Discussion and conclusions

The field and petrological observations data presented in this paper indicate that in the Ayakhtinsk aureole (1) the grade of contact metamorphism ranges from chloritoid to sillimanite–alkali feldspar zone; (2) the stability field of the assemblage chloritoid + biotite has a restricted temperature interval within the biotite zone; (3) chloritoid + biotite assemblages give way up-grade to garnet + chlorite assemblages; (4) chloritoid + biotite + andalusite assemblages occupy a restricted temperature interval within the andalusite zone; (5) garnet + chlorite assemblages give way to cordierite + biotite parageneses with increasing grade; (6) cordierite + garnet + muscovite assemblage is found in the lower cordierite zone; (7) staurolite-bearing assemblages are absent in this mineral sequence; (8) prograde sillimanite and alkali feldspar occur in the andalusite stability field at lower grade than the breakdown of muscovite + quartz.

7.1. Comparison of natural sequences with petrogenetic grids and implications for contact metamorphism of Fe- and Al-rich graphitic metapelites in the study area

The petrological investigation from this study and other contact aureoles provides information that enables us to assess the validity of various petrogenetic

grids for mineral assemblages in the low-pressure part of $P–T$ space. Consideration of the relative relationships between the natural assemblages and the various alternative petrogenetic grids was done by comparing the prograde succession of natural assemblages (the metamorphic zonal sequences) with the $P–T$ arrangement of reactions on various grids. For this purpose, we have chosen the most frequently cited petrogenetic grids for metapelites with markedly different topologies, particularly with respect to the controversial assemblage chloritoid + biotite (Harte and Hudson, 1979; Spear and Cheney, 1989; Powell and Holland, 1990).

The first appearance of chloritoid + biotite assemblage at the expense of chlorite + muscovite within the Ayakhtinsk contact aureole and the $P–T$ location corresponding to this reaction agree with Spear and Cheney's (1989) petrogenetic grid for KFMASH system. Spear and Cheney's petrogenetic grid for KFMASH system shows that chloritoid + biotite assemblage is stable on the low temperature side of the reaction chloritoid + biotite = garnet + chlorite and gives way up-grade to garnet + chlorite assemblages, opposite to that proposed by Harte and Hudson grid (1979). The differences between the various grids lie also in the treatment of markedly different stability limits of the assemblage chloritoid + biotite. One is based on the KFMASH grid of Harte and Hudson (1979), in which chloritoid + biotite is stable over a narrow temperature interval at relatively low pressure, and the other on the KFMASH grids of Spear and Cheney (1989) and Wang and Spear (1991), in which this assemblage is stable over wide ranges of pressure and temperature. Powell and Holland (1990) use internally consistent thermodynamic data to calculate petrogenetic grids for pelitic rocks and show that addition of a small amounts of Fe^{3+} in natural phases gives a stability field for chloritoid + biotite on the high temperature side of garnet + chlorite. While their $P–T$ diagram extends to $T = 520$ °C and 4 kbar, assuming that the reaction Grt + Chl = Cld + Bt is linear, biotite + chloritoid + andalusite should be stable at $P > 3$ kbar and $T > 460$ °C, consistent with our data. Spear and Cheney's (1989) and Wang and Spear's (1991) grids also predict that chloritoid + biotite should be stable in the andalusite field in the KFMASH system over wide range of temperatures at low grades, and that garnet + chlorite assemblages are restricted to a wedge in $P–T$ space at pressure > 0.5 kbar. A restricted temperature interval of the chloritoid + biotite stability field at low pressure predicted by Harte and Hudson's (1979) and Powell and Holland's (1990) grids can be also explained in the framework of Spear and Cheney's grid. The addition of MnO to garnet expands the stability of garnet + chlorite relative to chloritoid + biotite to lower temperatures and higher pressures. Taking the measured Fe/(Fe + Mg) garnet value of 0.95 and Mn/Mn + Mg + Fe value of 0.2 for the divariant assemblage Ms + Qtz + Bt + Chl + Grt + Cld, Spear and Cheney's calibrated grid gives a limited temperature interval of the chloritoid + biotite stability field in the andalusite field of ~ 50 °C, in agreement with that obtained from this study and other contact aureoles with the mineral assemblages chloritoid + biotite and chloritoid + andalusite + biotite. Phase relations of low- to medium-grade metapelites and the influence of the extra component MnO on these phase relations in $P–T$ space have been a matter of debate in recent years (Spear and Cheney, 1989; Droop and Harte, 1995; Mahar et al, 1997). Droop and Harte (1995) showed that the Grt + Chl assemblage in the medium-pressure regionally metamorphosed pelites of the S.E.Tauern is on the low-T side of reaction (4): low-Mn Grt + Chl = Cld + Bt. Wang and Spear (1991) discussed the coexistence of chloritoid + biotite in regionally metamorphosed rocks of the Barrovian sequence from the tri-state area of the Taconic Range, USA. They concluded that chloritoid + biotite parageneses are more strongly controlled by bulk composition than by $P–T$ conditions of metamorphism, and that chloritoid + biotite should appear in pelites with Fe/(Fe + Mg + Mn) > ~ 0.6. In contrast, garnet + chlorite should occur in rocks where Mg/(Mg + Fe + Mn) > 0.5. In rocks of intermediate bulk composition, it is possible to observe garnet + chlorite at low grade, followed by chloritoid + biotite at intermediate grade, followed by garnet + chlorite at higher grade. According to Wang and Spear (1991), this can happen if the effective Mn content of the rocks decreases with increasing temperature because of the fractionation of Mn into growing garnet porphyroblasts. Petrological and textural data from this study provide evidence in support of the KFMASH configuration of Spear and Cheney. Despite the difficulties inher-

ent to the presence of additional components, the petrogenetic grid of the KFMASH system of Spear and Cheney (1989) agrees well with the sequence of mineral reactions and assemblages found in the metapelites of the Ayakhtinsk contact aureole. We conclude that the formation of chloritoid atypical for thermal metamorphism at low pressure (< 1.5 kbar) and the stability of the rare mineral assemblages chloritoid + biotite and chloritoid + biotite + andalusite within contact aureoles can be explained by a combination of low pressure (≥ 3 kbar) and Fe- and Al-rich rich bulk-rock compositions.

Another feature that characterizes this contact metamorphic aureole is the local occurrence of garnet + cordierite + muscovite assemblages. Based on the observed mineral assemblages, this paragenesis is considered to be unstable in the pure KFMASH system (Pattison and Tracy, 1991). The Harte and Hudson (1979) grid does not allow the mutual compatibility of cordierite + garnet. Spear and Cheney's (1989) grid predicts that garnet + cordierite should only be stable in the K-feldspar field; however, a sizeable stability field for garnet + cordierite + muscovite occurs if MnO is taken into consideration. In the petrogenetic grid of Powell and Holland (1990) there are reactions involving garnet + cordierite with decreasing temperature and pressure until andalusite + chlorite = garnet + cordierite terminates in KFASH invariant point at about 520 °C and 2 kbar. However, at temperatures lower than 575 °C, garnet + cordierite can only occur in compositions more aluminous than garnet + chlorite, and only in Fe-rich compositions. This is consistent with the bulk composition of the hornfelses studied. Examination of Spear and Cheney's (1989) grid reveals that the P–T stability field for garnet + chlorite + andalusite + muscovite is quite restricted in the KFMASH system and the occurrence of this assemblage cannot be accommodated solely by KFMASH phase relations in the grid. This feature can be explained, in part, by examination of Fe/(Fe + Mg) contours in Fig. 3 of Spear and Cheney (1989). At low pressures (< 3 kbar), isopleths of Fe/(Fe + Mg) in garnet in the assemblage garnet + chlorite + andalusite + biotite are restricted to values > 0.9; consequently, this paragenesis will occur in Fe-rich compositions. Taking into consideration that some occurrences of these assemblages from low-pressure contact and high-pressure regional metamorphic settings have been reported, we conclude that the appearance and stability of cordierite + garnet + muscovite mineral assemblage as well as garnet + andalusite + chlorite + muscovite result from the stabilizing effect of Mn on garnet and from the Fe- and Al-rich composition of the rocks.

Another feature that characterizes the Ayakhtinsk contact aureole is the absence of staurolite-bearing assemblages and the abundance of assemblages containing cordierite and andalusite + biotite at low to intermediate grade in the aureole. There is no evidence for the chloritoid + andalusite = staurolite + chlorite or garnet + chlorite = staurolite + biotite reactions predicted by many grids. However, staurolite-bearing assemblages are favoured in Fe- and Al-rich bulk compositions at $P > 2$ kbar. Within the aureole studied, the muscovite + chlorite assemblages give way to andalusite + biotite parageneses with increasing grade. Garnet + chlorite assemblages are found at grades above the andalusite zone, but their stability is restricted with increasing grade. The addition of MnO to garnet expands the terminal stability of the assemblage garnet + chlorite relative to chloritoid + biotite to lower temperatures and that of garnet + chlorite relative to staurolite + biotite to higher temperatures, as modelled in the petrogenetic grid of Spear and Cheney (1989). At $P = 3$ kbar and $T = 560$ °C garnet + chlorite assemblages give way to biotite + cordierite parageneses, corresponding closely to the P–T location of the Chl + Grt = Bt + Crd reaction in the petrogenetic grid of Powell and Holland (1990). Thereafter, a narrow lens-shaped stability field for staurolite + biotite is entirely wedged out, and typical intermediate-grade andalusite + cordierite hornfelses appear in the study area. The observed metapelitic sequence from this study and in both low- and high-pressure regional metamorphic terrains show that sequence involved in breaking the garnet + chlorite join relative to the appearance of staurolite is of primary importance in the development of the staurolite-bearing parageneses. If the garnet + chlorite join is broken before the lower thermal stability of staurolite, then the paragenesis staurolite + biotite is observed before cordierite-bearing assemblages are encountered. However, if the garnet + chlorite join is broken after the lower thermal stability of staurolite, then no staurolite +

biotite parageneses can be stable, corresponding to the absence of staurolite-bearing assemblages from this study and other terranes.

Thus, natural assemblage data from this study provide information on the topology of the KFMASH grids for natural, Fe- and Al-rich graphitic pelites in the low-pressure part of P–T space, and are consistent with the KFMASH grid of Spear and Cheney (1989), extended by Wang and Spear (1991) to Mn-bearing compositions.

Acknowledgements

This research was supported by grants 00-05-65386 from the Russian Foundation of Basic Researches and the International Science Foundation (JAK-100) to I.I.L. The authors are greatly indebted to G. Droop, D. Pattison, B. Dutrow and J. Laird, for painstaking and well-disposed editing, valuable comments and criticism, that helped to significantly improve the arguments and the organization of the original manuscript. T. Horscroft is thanked for the careful editorial handling and constructive comments.

References

Albee, A.L., 1972. Metamorphism of pelitic schists: reaction relations of chloritoid and staurolite. Geological Society of America Bulletin 83, 3249–3268.

Aranovich, L.Ya., Podlesskii, K.K., 1989. Geothermobarometry of high-grade metapelites: simultaneously operating reactions. In: Daly, J.S., Cliff, R.A., Yardley, B.W.D. (Eds.), 1989. Evolution of Metamorphic Belts, vol. 43. Geological Society, London, pp. 45–61, Special Publication.

Atherton, M.P., 1980. The occurrence and implications of chloritoid in a contact aureole andalusite schists from Ardara, County Donegal. Journal of Earth Science, Royal Dublin Society 3, 101–109.

Barton, M.D., Ilchik, R.P., Marikos, M.A., 1991. Metasomatism. In: Kerrick, D.M. (Ed.), Contact Metamorphism. Reviews in Mineralogy, vol. 26. Mineralogical Society of America, Chelsea, Michigan, pp. 321–350.

Bird, G.W., Fawcett, J.J., 1973. Stability relations of Mg-chlorite, muscovite and quartz between 5 and 10 kb water pressure. Journal of Petrology 14, 415–428.

Bohlen, S.R., Montana, A.L., Kerrick, D.M., 1991. Precise determinations of the equilibria kyanite = sillimanite and kyanite = andalusite, and a revised triple point for Al_2SiO_5 polymorphs. American Mineralogist 76, 677–680.

Carey, J.W., 1995. A thermodynamic formulation of hydrous cordierite. Contribution to Mineralogy and Petrology 119, 155–165.

Carmichael, D.M., 1978. Metamorphic bathozones and bathograds: a measure of the depth of post-metamorphic uplift and erosion on the regional scale. American Journal of Science 278, 769–797.

Chatterjee, N.D., Johannes, W.S., 1974. Thermal stability and standard thermodynamic properties of synthetic $2M_1$-muscovite $KAl_2Al_3Si_3O_{10}(OH)_2$. Contributions to Mineralogy and Petrology 48, 89–114.

Chinner, G.A., 1967. Chloritoid and the isochemical character of Barrow's zones. Journal of Petrology 8, 268–282.

Connolly, J.A.D., Cesare, B., 1993. C–O–H–S fluid composition and oxygen fugasity in graphitic metapelites. Journal of Metamorphic Geology 11, 379–388.

Dazenko, V.M., 1984. Granitoid magmatism of the South-West edge of the Siberian platform. Nauka, Novosibirsk, 235 pp. (in Russian).

Dickenson, M.P., 1988. Local and regional differences in the chemical potential of water in amphibolite facies pelitic schists. Journal of Metamorphic Geology 6, 365–381.

Droop, G.T.R., Harte, B., 1995. The effect of Mn on the phase relations of medium-grade pelites: constraints from natural assemblages on petrogenetic grid topology. Journal of Petrology 36, 1549–1578.

Droop, G.T.R., Treloar, P.J., 1981. Pressures of metamorphism in the thermal aureole of the Etive granite complex. Scottish Journal of Geology 17, 85–102.

Duan, Z., Moller, N., Weare, J.H., 1992. An equation of state for the CH4–CO2–H2O system: I. Pure systems from 0 to 1000 °C and 0 to 8000 bar. Geochimica et Cosmochimica Acta 56, 2605–2617.

Evirgen, M.M., Ashworth, J.R., 1984. Andalusitic and kyanitic facies series in the central Menderes Massif, Turkey. Neues Jahrbuch der Mineralogie, Monatsshefte, pp. 219–227.

Ferry, J.M., 1976. P,T,f_{CO_2}, and f_{H_2O} during metamorphism of calcareous sediments in the Waterville-Vassalboro area, south-central Maine. Contributions to Mineralogy and Petrology 57, 119–143.

Ferry, J.M., 1980. A comparative study of geothermometers and geobarometers in pelitic schists from south-central Maine. American Mineralogist 65, 720–732.

Ferry, J.M., 1982. A comparative geochemical study of pelitic schists and metamorphosed carbonate rocks from south-central Maine, U.S.A. Contributions to Mineralogy and Petrology 80, 59–72.

Flinn, D., Key, R.M., Khoo, T.T., 1996. The chloritoid schists of Shetland and their thermal metamorphism. Scottish Journal of Geology 32, 67–82.

Foster Jr., C.T., 1977. Mass transfer in sillimanite-bearing pelitic schists near Rangeley, Maine. American Mineralogist 62, 727–746.

French, B.M., 1966. Some geological implications of equilibrium between graphite and C–H–O gas phase at high temperatures and pressures. Reviews of Geophysics 4, 223–253.

Frey, M., 1978. Progressive low-grade metamorphism of a black

shale formation, central Swiss Alps with special reference to pyrophyllite and margarite bearing assemblages. Journal of Petrology 19, 93–135.

Ganguly, J., 1969. Chloritoid stability and related paragenesis: theory, experiments and applications. American Journal of Sciences 267, 910–944.

Ghent, E.D., Stout, M.Z., 1981. Geobarometry and geothermometry of plagioclase–biotite–garnet–muscovite assemblages. Contributions to Mineralogy and Petrology 76, 92–97.

Grambling, J.A., 1986. A regional gradient in the composition of metamorphic fluids in pelitic schists, Pecos Baldy, New Mexico. Contributions to Mineralogy and Petrology 94, 149–164.

Green, N.L., Usdansky, S.I., 1986a. Ternary-feldspar mixing relations and thermobarometry. American Mineralogist 71, 1100–1108.

Green, N.L., Usdansky, S.I., 1986b. Toward a practical plagioclase–muscovite thermometer. American Mineralogist 71, 1109–1117.

Greenwood, H.J., 1975. Buffering of pore fluids by metamorphic reactions. American Journal of Science 275, 573–593.

Guidotti, C.V., 1984. Micas in metamorphic rocks. In: Bailey, S.W. (Ed.), Micas. Reviews in Mineralogy, vol. 13. Mineralogical Society of America, Chelsea, Michigan, pp. 357–467.

Halferdahl, L.B., 1961. Chloritoid: its composition, X-ray and optical properties, stability and occurrence. Journal of Petrology 2, 49–135.

Harte, B., 1975. Determination of a pelite petrogenetic grid for the eastern Scottish Dalradian. Yearbook, vol. 74. Carnegie Institution of Washington, Washington, DC, pp. 438–446.

Harte, B., Hudson, N.F.C., 1979. Pelite facies series and the temperatures and pressures of Dalradian metamorphism in eastern Scotland. In: Harris, A.L., Holland, C.H., Leake, B.E. (Eds.), The Caledonides of the British Isles. Reviewed. Geological Society Special Publication, 8. The Geological Society, London, pp. 323–337.

Hodges, K.V., Crowley, P.D., 1985. Error estimation and empirical geothermobarometry for pelitic system. American Mineralogist 70, 702–709.

Hoisch, T.D., 1989. A muscovite–biotite geothermometer. American Mineralogist 74, 565–572.

Hoisch, T.D., 1990. Empirical calibration of six geobarometers for the mineral assemblage quartz + muscovite + biotite + plagioclase + garnet. Contributions to Mineralogy and Petrology 104, 225–234.

Hoisch, T.D., 1991. Equilibria within the mineral assemblage quartz + muscovite + biotite + garnet + plagioclase and implications for the mixing properties of octahedrally coordinated cations in muscovite and biotite. Contributions to Mineralogy and Petrology 108, 43–54.

Holdaway, M.J., 1971. Stability of andalusite and the aluminum silicate phase diagram. American Journal of Sciences 371, 97–131.

Holdaway, M.J., 1978. Significance of chloritoid and staurolite-bearing rocks in the Picuris Range, New Mexico. Geological Society of American Bulletin 89, 1404–1414.

Holdaway, M.J., Lee, S.M., 1977. Fe–Mg cordierite stability in high-grade pelitic rocks based on experimental, theoretical, and natural observations. Contribution to Mineralogy and Petrology 63, 175–198.

Holdaway, M.J., Dutrow, B.L., Hinton, R.W., 1988. Devonian and Carboniferous metamorphism in west-central Maine: the muscovite-almandine geobarometer and the staurolite problem revisited. American Mineralogist 73, 20–47.

Holland, T.J.B., Powell, R., 1990. An enlarged and updated internally consistent thermodynamic dataset with uncertainties and correlations: the system K_2O–Na_2O–CaO–MgO–FeO–Fe_2O_3–Al_2O_3–TiO_2–SiO_2–C–H_2–O_2. Journal of Metamorphic Geology 6, 89–124.

Hoschek, G., 1969. The stability of staurolite and chloritoid and their significance in metamorphism of pelitic rocks. Contribution to Mineralogy and Petrology 22, 208–232.

Hsu, L.G., 1968. Selected phase relationships in the system Al–Mn–Fe–Si–O–OH: a model for garnet equilibria. Journal of Petrology 9, 40–83.

James, H.L., Howland, A.L., 1955. Mineral facies in iron- and silica-rich rocks. Geological Society of America Bulletin 66, 1580–1581.

Johannes, W., 1985. The significance of experimental studies for the formation of migmatites. In: Ashworth, J.R. (Ed.), Migmatites. Blackie, Glasgow, pp. 36–85.

Kaneko, Y., Miyano, T., 1990. Contact metamorphism by the bushveld complex in the northeastern Transvaal, South Africa. Journal of Mineralogy, Petrology and Economic Geology 85, 66–81.

Kepezhinskas, K.B., 1977. Paragenetic analysis and petrochemistry of middle-grade metapelites. Nauka, Novosibirsk, 196 pp. (in Russian).

Kerrick, D.M., Heninger, S.G., 1984. The andalusite–sillimanite equilibrium revisited. Geol. Soc. Am. Abs. Prog. 16, 558.

Kerrick, D.M., Jacobs, C.K., 1981. A modified Redlich-Kwong equation for H_2O,CO_2 and H_2O–CO_2 mixtures at elevated pressures and temperatures. American Journal of Science 281, 735–767.

Kerrick, D.M., Woodsworth, G.J., 1989. Aluminium silicates in the Mount Raleigh pendant, British Columbia. Journal of Metamorphic Geology 7, 547–563.

Kolobov, V.Y., Likhanov, I.I., Reverdatto, V.V., 1992. Contact-metamorphic rocks. In: Dobretsov, N.L. (Ed.), Classification and Nomenclature of Metamorphic Rocks. Nauka, Novosibirsk, pp. 77–97.

Korikovskii, S.P., 1979. The Facies of Metapelitic Metamorphism. Nauka, Moscow, 247 pp. (in Russian).

Kotov, N.V., 1986. Thermodynamic conditions of late diagenesis and initial metamorphism. In: Bulakh, A.G. (Ed.), Clay Minerals in Lithogenesis. Nauka, Moscow, pp. 90–103 (in Russian).

Kozlov, P.S., 1994. Petrology, petrochemistry and metamorphism of rocks in the Transangara region of the Yenisey Ridge. Doctoral Thesis, Novosibirsk University, Russia (in Russian).

Kretz, R., 1983. Symbols for rock-forming minerals. American Mineralogist 68, 277–279.

Labotka, T.C., 1981. Petrology of an andalusite-type regional metamorphic terrain, Panamint Mountains, California. Journal of Petrology 22, 261–296.

Likhanov, I.I., 1988a. Chloritoid, staurolite and gedrite of the

high-alumina hornfelses of the Karatash pluton. International Geological Review 30, 868–877.

Likhanov, I.I., 1988b. Evolution of chemical composition in metapelite minerals during low-grade contact metamorphism of the Karatash massif. International Geological Review 30, 878–888.

Likhanov, I.I., 1989. Metamorphic fluid composition gradients in metapelitic hornfelses. Geochemistry International 26, 132–137.

Likhanov, I.I., Reverdatto, V.V., Memmi, I., 1994. Short-range mobilization of elements in the biotite zone of contact aureole of the Kharlovo gabbro massif (Russia). European Journal of Mineralogy 6, 133–144.

Likhanov, I.I., Reverdatto, V.V., Memmi, I., 1995. The origin of arfvedsonite in metabasites from the contact aureole of the Kharlovo gabbro intrusion (Russia). European Journal of Mineralogy 7, 379–389.

Likhanov, I.I., Sheplev, V.S., Reverdatto, V.V., Kozlov, P.S., 1998. Contact metamorphism of ferriferous metapelites at relatively high pressure in the Transangarian region of Yenisei Ridge. Transactions (Doklady) of the Russian Academy of Sciences 362, 673–676 (in Russian).

Likhanov, I.I., Sheplev, V.S., Reverdatto, V.V., Kozlov, P.S., Kireev, A.D., 1999. The isochemical nature of the contact metamorphism of high-alumina metapelites in the Ayakhta granitoid massif, Yenisei Ridge. Russian Geology and Geophysics 40, 91–98.

Likhanov, I.I., Polyansky, O.P., Reverdatto, V.V., Kozlov, P.S., Verschinin, A.E., Krebs, M., Memmi, I., 2000. Andalusite-kyanite transformation at the pressure increase and extremely low geothermal gradient conditions during overthrusting in the Transangarian region of the Yenisey Ridge. Transactions (Doclady) of the Russian Academy of Sciences 375, 509–513 (in Russian).

Mahar, E.M., Baker, J.M., Powell, R., Holland, T.J.B., Howell, N., 1997. The effect of Mn on mineral stability in metapelites. Journal of Metamorphic Geology 15, 223–238.

Naggar, M.H., Atherton, M.P., 1970. The composition and metamorphic history of some aluminium silicate-bearing rocks from the aureoles of the Donegal Granites. Journal of Petrology 11, 549–589.

Nockolds, S.R., Knox, R.W., Chinner, G.A., 1978. Petrology for Students. Cambridge Univ. Press, Cambridge, 340 pp.

Ohmoto, H., Kerrick, D.M., 1977. Devolatilization equilibria in graphitic system. American Journal of Science 277, 1013–1044.

Okuyama-Kusunose, Y., 1994. Phase relations in andalusite–sillimanite type Fe-rich aluminous metapelites: Tono contact metamorphic aureole, northeast Japan. Journal of Metamorphic Geology 12, 153–168.

Pattison, D.R.M., 1989. P–T conditions and the influence of graphite on pelitic phase relations in the Ballachulish aureole, Scotland. Journal of Petrology 30, 1219–1244.

Pattison, D.R.M., 1992. Stability of andalusite and sillimanite and the Al_2SiO_5 triple point: constraints from the Ballachulish aureole, Scotland. Journal of Geology 100, 423–446.

Pattison, D.R.M., Tracy, R.J., 1991. Phase equilibria and thermobarometry of metapelites. In: Kerrick, D.M. (Ed.), Contact Metamorphism. Reviews in Mineralogy, vol. 26. Mineralogical Society of America, Chelsea, Michigan, pp. 105–206.

Perchuk, L.L., 1991. Derivation of a thermodynamically consistent set of geothermometers and geobarometers for metamorphic and magmatic rocks. In: Perchuk, L.L. (Ed.), Progress in Metamorphic and Magmatic Petrology. Cambridge Univ. Press, Cambridge, pp. 93–112.

Phillips, G.N., 1987. The metamorphism of the Witwatersrand goldfields. Journal of Metamorphic Geology 5, 307–322.

Powell, R., Holland, T.J.B., 1985. An internally consistent thermodynamic dataset with uncertainties and correlations: 1. Methods and a worked example. Journal of Metamorphic Geology 3, 327–342.

Powell, R., Holland, T.J.B., 1988. An internally consistent thermodynamic dataset with uncertainties and correlations: 3. Applications to geobarometry, worked examples and computer program. Journal of Metamorphic Geology 6, 173–204.

Powell, R., Holland, T.J.B., 1990. Calculated mineral equilibria in the pelite system, KFMASH (K_2O–FeO–MgO–Al_2O_3–SiO_2–H_2O). American Mineralogist 75, 367–380.

Powell, R., Holland, T.J.B., 1994. Optimal geothermometry and geobarometry. American Mineralogist 79, 120–133.

Powell, R., Holland, T.J.B., 1998. An internally consistent thermodynamic data set for phases of petrological interest. Journal of Metamorphic Geology 16, 309–343.

Reverdatto, V.V., 1973. The Facies of Contact Metamorphism. Australian National University Pub. 203, Canberra, 198 pp.

Reverdatto, V.V., Sharapov, V.N., Lavrent'ev, Yu.G., Pokachalova, O.S., 1974. Investigations in isochemical contact metamorphism. Contributions to Mineralogy and Petrology 48, 287–299.

Richardson, S.W., 1968. Staurolite stability in a part of the system Fe–Al–Si–O–H. Journal of Petrology 9, 467–488.

Richardson, S.W., Gilbert, M.C., Bell, P.M., 1969. Experimental determination of kyanite–andalusite and andalusite–sillimanite equilibria: the aluminum silicate triple point. American Journal of Sciences 267, 259–272.

Skippen, J.B., Gunter, A.E., 1996. The thermodynamic properties of H_2O in magnesian and iron cordierite. Contribution to Mineralogy and Petrology 124, 82–89.

Seifert, F., 1970. Low temperature compatibility relations of cordierite in haplopelites of the system K_2O–MgO–Al_2O_3–SiO_2–H_2O. Journal of Petrology 11, 73–99.

Shaw, D.M., 1956. Geochemistry of pelitic rocks: Part III. Major elements and general geochemistry. Geological Society America Bulletin 67, 913–934.

Spear, F.S., 1993. Metamorphic phase equilibria and pressure–temperature–time paths. Mineralogical Society of America, Washington, 799 pp.

Spear, F.S., Cheney, J.T., 1989. A petrogenetic grid for pelitic schists in the system SiO_2–Al_2O_3–FeO–MgO–K_2O–H_2O. Contributions to Mineralogy and Petrology 101, 149–164.

Spear, F.S., Ferry, J.M., Rumble III, D., 1982. Analytical formulation of phase equilibria: the Gibbs Method. In: Ferry, J.M. (Ed.), Characterization of Metamorphism through Mineral Equilibria. Reviews in Mineralogy, 10, Mineralogical Society of America, Chelsea, Michigan, pp. 105–152.

Symmes, G.H., Ferry, J.M., 1992. The effect of whole-rock MnO

content on the stability of garnet in pelitic schists during metamorphism. Journal of Metamorphic Geology 10, 221–237.

Thompson Jr., J.B., 1957. The graphical analysis of mineral assemblages in pelitic schists. American Mineralogist 42, 842–858.

Thompson, A.B., 1976. Mineral reactions in pelitic rocks: II. Calculation of some P–T–X(Fe–Mg) phase relations. American Journal of Science 276, 425–454.

Thompson, J.B., Norton, S.A., 1968. Paleozoic regional metamorphism in New England and adjacent areas. In: Zen, E-an (Ed.), Studies of Appalachian Geology: Northern and Maritime. Interscience Publisher, New York, pp. 319–327.

Tuttle, O.F., Bowen, N.L., 1958. Origin of granite in the light of experimental studies in the system $NaAlSi_3O8$–$KAlSi_3O8$–SiO_2–H_2O. Geological Society of America Memoir 74, 54–63.

Vernon, R.H., 1977. Relationships between microstructural and metamorphic assemblages. Tectonophysics 39, 439–452.

Urbakh, V.Y., 1964. Biometrical Methods. Mir, Moscow, 264 pp. (in Russian).

Wang, P., Spear, F.S., 1991. A field and theoretical analysis of garnet + chlorite + chloritoid + biotite assemblages from the tri-state (MA,CT,NY) area, U. S. A. Contributions to Mineralogy and Petrology 106, 217–235.

Whitney, D.L., Mechum, T.A., Kuehner, S.M., Dilek, Y.R., 1996. Progressive metamorphism of pelitic rocks from protolith to granulite facies, Dutchess County, New York, USA: constraints on the timing of fluid infiltration during regional metamorphism. J. Metamorphic Geol. 14, 163–181.

Yardley, B.W.D., 1977. Relationship between the chemical and modal compositions of metapelites from Connemara, Ireland. Lithos 10, 235–242.